M.S-V., and the Grant for Comprehensive Research on Disability Health and Welfare (H24-002) from the Japan Ministry of Health and Labour Science Research to H.M.

Mr Mori is a medical technologist and is enrolled in the PhD program in the Department of Microbiology, Faculty of Medicine, Oita University, Japan. His research interest is molecular epidemiology of viruses.

References

1. Granerod J, Ambrose HE, Davies NW, Clewley JP, Walsh AL, Morgan D, et al. Causes of encephalitis and differences in their clinical presentations in England: a multicentre, population-based prospective study. Lancet Infect Dis. 2010;10:835–44. http://dx.doi.org/10.1016/S1473-3099(10)70222-X
2. Huppatz C, Durrheim DN, Levi C, Dalton C, Williams D, Clements MS, et al. Etiology of encephalitis in Australia, 1990–2007. Emerg Infect Dis. 2009;15:1359–65. http://dx.doi.org/10.3201/eid1509.081540
3. Mitui MT, Shahnawaz Bin Tabib SM, Matsumoto T, Khanam W, Ahmed S, Mori D, et al. Detection of human bocavirus in the cerebrospinal fluid of children with encephalitis. Clin Infect Dis. 2012;54:964–7. http://dx.doi.org/10.1093/cid/cir957
4. Han TH, Kim CH, Park SH, Chung JY, Hwang ES. Detection of human parechoviruses in children with gastroenteritis in South Korea. Arch Virol. 2011;156:1471–5. http://dx.doi.org/10.1007/s00705-011-0995-y
5. Allander T, Tammi MT, Eriksson M, Bjerkner A, Tiveljung-Lindell A, Andersson B. Cloning of a human parvovirus by molecular screening of respiratory tract samples. Proc Natl Acad Sci U S A. 2005;102:12891–6. http://dx.doi.org/10.1073/pnas.0504666102
6. Takano S, Takahashi Y, Kishi H, Taguchi Y, Takashima S, Tanaka K, et al. Detection of autoantibody against extracellular epitopes of *N*-methyl-D-aspartate receptor by cell-based assay. Neurosci Res. 2011;71:294–302. http://dx.doi.org/10.1016/j.neures.2011.07.1834
7. Kantola K, Hedman L, Arthur J, Alibeto A, Delwart E, Jartti T, et al. Seroepidemiology of human bocaviruses 1–4. J Infect Dis. 2011;204:1403–12. http://dx.doi.org/10.1093/infdis/jir525
8. Zhang Z, Zheng Z, Luo H, Meng J, Li H, Li Q, et al. Human bocavirus NP1 inhibits IFN-beta production by blocking association of IFN regulatory factor 3 with IFNB promoter. J Immunol. 2012;189:1144–53. http://dx.doi.org/10.4049/jimmunol.1200096
9. Dupuis M, Hull R, Wang H, Nattanmai S, Glasheen B, Fusco H, et al. Molecular detection of viral causes of encephalitis and meningitis in New York State. J Med Virol. 2011;83:2172–81. http://dx.doi.org/10.1002/jmv.22169
10. Gable MS, Sheriff H, Dalmau J, Tilley DH, Glaser CA. The frequency of autoimmune *N*-methyl-D-aspartate receptor encephalitis surpasses that of individual viral etiologies in young individuals enrolled in the California Encephalitis Project. Clin Infect Dis. 2012;54:899–904. http://dx.doi.org/10.1093/cid/cir1038
11. Dalmau J, Lancaster E, Martinez-Hernandez E, Rosenfeld MR, Balice-Gordon R. Clinical experience and laboratory investigations in patients with anti-NMDAR encephalitis. Lancet Neurol. 2011;10:63–74. http://dx.doi.org/10.1016/S1474-4422(10)70253-2
12. Soares CN, Cabral-Castro MJ, Peralta JM, de Freitas MR, Zalis M, Puccioni-Sohler M. Review of the etiologies of viral meningitis and encephalitis in a dengue endemic region. J Neurol Sci. 2011;303:75–9. http://dx.doi.org/10.1016/j.jns.2011.01.012
13. Tavakoli NP, Wang H, Nattanmai S, Dupuis M, Fusco H, Hull R. Detection and typing of enteroviruses from CSF specimens from patients diagnosed with meningitis/encephalitis. J Clin Virol. 2008;43:207–11. http://dx.doi.org/10.1016/j.jcv.2008.06.016
14. Frange P, Peffault de Latour R, Arnaud C, Boddaert N, Oualha M, Avettand-Fenoel V, et al. Adenoviral infection presenting as an isolated central nervous system disease without detectable viremia in two children after stem cell transplantation. J Clin Microbiol. 2011;49:2361–4. http://dx.doi.org/10.1128/JCM.00080-11
15. Straussberg R, Harel L, Levy Y, Amir J. A syndrome of transient encephalopathy associated with adenovirus infection. Pediatrics. 2001;107:E69. http://dx.doi.org/10.1542/peds.107.5.e69

Address for correspondence: Kamruddin Ahmed, Research Promotion Institute, Oita University, Yufu 879-5593, Oita, Japan; email: ahmed@oita-u.ac.jp

OPEN ACCESS Freely available online

PLoS one

Role of Serine Racemase in Behavioral Sensitization in Mice after Repeated Administration of Methamphetamine

Mao Horio[1], Mami Kohno[1], Yuko Fujita[1], Tamaki Ishima[1], Ran Inoue[2], Hisashi Mori[2], Kenji Hashimoto[1]*

1 Division of Clinical Neuroscience, Chiba University Center for Forensic Mental Health, Chiba, Japan, 2 Department of Molecular Neuroscience, Toyama University Graduate School of Medicine, Toyama, Japan

Abstract

Background: The N-methyl-D-aspartate (NMDA) receptors play a role in behavioral abnormalities observed after administration of the psychostimulant, methamphetamine (METH). Serine racemase (SRR) is an enzyme which synthesizes D-serine, an endogenous co-agonist of NMDA receptors. Using Srr knock-out (KO) mice, we investigated the role of SRR on METH-induced behavioral abnormalities in mice.

Methodology/Principal Findings: Evaluations of behavior in acute hyperlocomotion, behavioral sensitization, and conditioned place preference (CPP) were performed. The role of SRR on the release of dopamine (DA) in the nucleus accumbens after administration of METH was examined using in vivo microdialysis technique. Additionally, phosphorylation levels of ERK1/2 proteins in the striatum, frontal cortex and hippocampus were examined using Western blot analysis. Acute hyperlocomotion after a single administration of METH (3 mg/kg) was comparable between wild-type (WT) and Srr-KO mice. However, repeated administration of METH (3 mg/kg/day, once daily for 5 days) resulted in behavioral sensitization in WT, but not Srr-KO mice. Pretreatment with D-serine (900 mg/kg, 30 min prior to each METH treatment) did not affect the development of behavioral sensitization after repeated METH administration. In the CPP paradigm, METH-induced rewarding effects were demonstrable in both WT and Srr-KO mice. In vivo microdialysis study showed that METH (1 mg/kg)induced DA release in the nucleus accumbens of Srr-KO mice previously treated with METH was significantly lower than that of the WT mice previously treated with METH. Interestingly, a single administration of METH (3 mg/kg) significantly increased the phosphorylation status of ERK1/2 in the striatum of WT, but not Srr-KO mice.

Conclusions/Significance:These findings suggest first, that SRR plays a role in the development of behavioral sensitization in mice after repeated administration of METH, and second that phosphorylation of ERK1/2 by METH may contribute to the development of this sensitization as seen in WT but not Srr-KO mice.

Citation: Horio M, Kohno M, Fujita Y, Ishima T, Inoue R, et al. (2012) Role of Serine Racemase in Behavioral Sensitization in Mice after Repeated Administration of Methamphetamine. PLoS ONE 7(4): e35494. doi:10.1371/journal.pone.0035494

Editor: Bernard Le Foll, Centre for Addiction and Mental Health, Canada

Received February 15, 2012; Accepted March 20, 2012; Published April 18, 2012

Funding: This study was supported by grants from Grants-in-Aid for Scientific Research of Japan Society for the Promotion of Science, Japan (to K.H.) and Intramural Research Grant for Neurological and Psychiatric Disorders of National Center of Neurology and Psychiatry (NCNP), Japan (to K.H.). The funders had no role in study design, data collection and analysis, decision to publish, or preparation of the manuscript.

Competing Interests: The authors have declared that no competing interests exist.

* E-mail: hashimoto@faculty.chiba-u.jp

Introduction

Abuse of the psychostimulant methamphetamine (METH) is a serious and growing worldwide problem. Long-term use of METH results in addiction, which is characterized by compulsive drugseeking and drug use, with accompanying functional and molecular changes in the brain. Addiction to METH is also a major public health concern, since chronic use is associated with major medical, psychiatric, cognitive, socioeconomic and legal consequence [1,2]. Repeated consumption of METH can induce a psychotic state (METH psychosis), with symptoms resembling those of paranoid-type schizophrenia [3–5]. There is currently no standard pharmacological treatment for the wide range of symptoms associated with METH abuse [1,6,7]. Moreover, the precise molecular and cellular mechanisms underlying the longterm effects of METH in the brain, remain undetermined [1,8,9].

METH causes neurochemical changes in several areas of the brain via the dopaminergic system, and consequently via glutamatergic neurotransmission [10–13]. Repeated administration of this psychostimulant to rodents, produces long-term behavioral changes, including behavioral sensitization and dependence [14,15]. The N-methyl-D-aspartate (NMDA) receptor antagonist MK-801 blocks the development of METH (or amphetamine)-induced behavioral sensitization [16–20]. It is therefore likely that the NMDA receptor plays a role in the mechanisms of behavioral sensitization seen in rodents after repeated administration of psychostimulants, such as METH and amphetamine.

D-Serine is an endogenous co-agonist at the glycine-binding site of the NMDA receptor subunit, GluN1 [21–23]. D-Serine is

synthesized from L-serine by the enzyme, serine racemase (SRR), and shows a similar localization within the brain to D-serine [24,25]. Studies using Srr knockout (Srr-KO) mice show that SRR is predominantly localized to forebrain neurons [26] and that levels of D-serine in the forebrain are 10–20% of wild-type (WT) mice [27–29], suggesting that SSR provides the main catalysis for D-serine production in the forebrain. In addition, we reported that NMDA-induced neurotoxicity is significantly attenuated in the brains of Srr-KO mice, suggesting that D-serine controls the extent of NMDA receptor-mediated neurotoxic insults [27]. It is therefore likely that D-serine produced by SSR, plays an important role in NMDA receptor-mediated neurotransmission in the brain.

To study the role of SRR in METH-induced behavioral abnormalities, we evaluated behavioral performances in acute hyperlocomotion, development of behavioral sensitization, and conditioned place preference (CPP) in WT and Srr-KO mice, after the administration of METH. Furthermore, we examined the role of SRR on the dopamine (DA) release in the nucleus accumbens after administration of METH using in vivo microdialysis technique. In addition, we examined whether METH administration altered phosphorylation levels of ERK1/2 in the striatum, since ERK1/2 phosphorylation contributes to the development of behavioral sensitization by psychostimulants [30,31].

Results

METH-induced acute hyperlocomotion

A single dose of METH (3 mg/kg, s.c.), but not METH (1 mg/ kg, s.c.), markedly increased locomotion in both WT and Srr-KO mice. Two-way ANOVA analysis revealed significant drug treatment effects for METH-induced locomotor responses [genotype: F (1,48) =1.12, p = 0.29; drug treatment: F (2,48) = 26.97, p,0.001], with no genotype x drug treatment interaction (F (2,48) = 0.27, p = 0.77). Subsequent one-way ANOVA followed post hoc Bonferroni/Dun test indicated that METH (3 mg/kg) significantly increased locomotion in both WT and Srr-KO mice (WT: p =0.002; Srr-KO: p,0.001 as compared to saline treated group) (Figure 1).

Next, we examined whether pretreatment with D-serine affected METH-induced acute hyperlocomotion in mice. Thirty minutes after a single oral dose of D-serine (900 mg/kg) or vehicle (10 ml/kg), mice were given a s.c dose of METH (3 mg/ kg). Two-way ANOVA analysis revealed that D-serine had no significant effect on METH-induced acute hyperlocomotion [genotype: F (1,24) = 6.00, p = 0.02; drug treatment: F (1,24) = 0.02, p= 0.88; interaction: F(1,24) =0.02, p = 0.89]. Student's t-test indicated that pretreatment with D-serine (900 mg/ kg) had no effect on METH-induced hyperlocomotion in either WT or Srr-KO mice (WT: t =0.26, p = 0.80; Srr-KO: t =0.006, p = 1.00) (Figure S1).

METH-induced behavioral sensitization

Two-way ANOVA analysis revealed a significant effect for METH-induced hyperlocomotion [genotype: F (1,34) =7.97, p = 0.008; drug treatment: F (1,34) =33.46, p,0.001; interaction: F (1,34) =11.83, p =0.002]. One-way ANOVA revealed a significant (F (3,34) =18.37, p,0.001) difference among the four groups. Challenging mice with a low dose of METH (1 mg/kg) significantly (p,0.001) increased METH -induced hyperlocomotion in WT mice previously treated with METH (3 mg/kg/day over 5 consecutive days), compared with saline treated WT mice (Figure 2). In contrast, METH (1 mg/kg) -induced hyperlocomotion was comparable between Srr-KO mice previously treated with METH (3 mg/kg/day over 5 consecutive days) or saline (Figure 2), indicating a lack of METH-induced behavioral sensitization in Srr-KO mice. Furthermore, locomotion in WT mice pretreated with METH (3 mg/kg/day for 5 consecutive days) was significantly (p = 0.001) higher than seen in Srr-KO mice pretreated with METH (Figure 2). These results indicated that behavioral sensitization occurred in WT but not Srr-KO mice after repeated administration of METH.

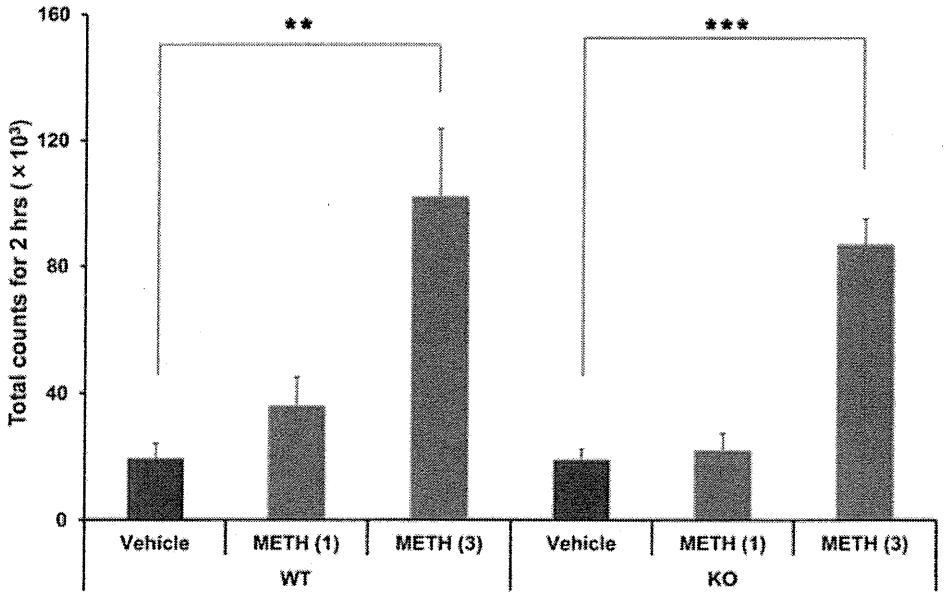

Figure 1. METH-induced acute hyperlocomotion in WT and Srr-KO mice. METH (1 or 3 mg/kg) or vehicle (saline; 10 ml/kg) was administered s.c. to WT and Srr-KO mice. Behavior (locomotion) was evaluated as described in the Methods and Materials. Each value is the mean 6 SEM (n = 8–10 per group). **p,0.01, ***p,0.001 as compared with the vehicle treated group.

doi:10.1371/journal.pone.0035494.g001

Figure 2. The development of behavioral sensitization in mice after repeated administration of METH. Mice were treated daily for 5 consecutive days with vehicle (10 ml/kg) or METH (3 mg/kg). Seven days after the final dosing, mice were given a lower dose of METH (1 mg/kg, s.c.). Locomotion in mice was

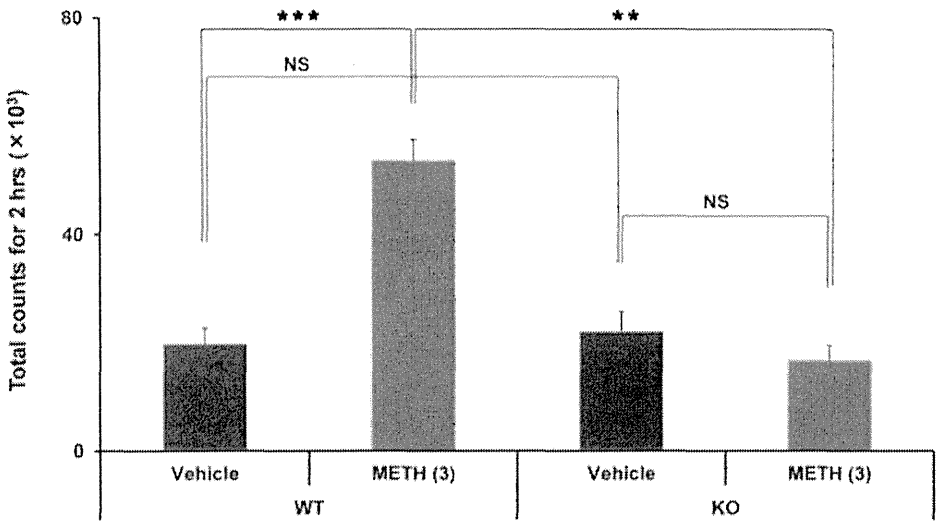

evaluated as described in the Methods and Materials. Each value is the mean 6 SEM (n = 9 or 10 per group). **p,0.01, ***p,0.001 as compared with the vehicle treated group (Bonferroni/Dunn method).
doi:10.1371/journal.pone.0035494.g002

To examine whether pretreatment with D-serine affected METH-induced behavioral sensitization in Srr-KO mice, mice were administered a single oral dose of D-serine (900 mg/kg/day) or vehicle (10 ml/kg/day) thirty minutes before dosing with METH (3 mg/kg/day). Two-way ANOVA analysis revealed a significant genotypic effect for METH-induced locomotion [genotype: F (1,24)= 27.17, p,0.001; drug treatment: F (1,24) = 1.31, p= 0.26], with no genotype x drug interaction (F (1,24) = 0.21, p = 0.65). One-way ANOVA revealed significant (F (3,24) = 9.562, p,0.001) differences among the four groups. Pretreatment with D-serine (900 mg/kg) showed no effect on METH (1 mg/kg)-induced locomotion in either WT or Srr-KO mice. In contrast, locomotion in WT mice pretreated with vehicle followed by METH (3 mg/kg) was significantly (p =0.015) higher than in Srr-KO mice treated in the same way (Figure S2), consistent with results in Figure 2. Furthermore, locomotion in WT mice pretreated with D-serine (900 mg/kg) followed by a larger dose of METH (3 mg/kg) was significantly (p= 0.003) higher than in Srr-KO mice treated in the same manner (Figure S2). These results showed that pretreatment of D-serine (900 mg/ kg) prior to each METH injection had no effect on METH (1 mg/ kg)-induced locomotion in WT and Srr-KO mice pretreated with METH.

METH-induced DA release in the nucleus accumbens

To explore how SRR contributes to METH-induced sensitization, we measured extracellular DA levels in the nucleus accumbens after administration of METH (1 mg/kg), using an in vivo microdialysis technique. A dose of METH (1 mg/kg, s.c.) caused a marked increase in extracellular DA levels in the nucleus accumbens of WT, not Srr-KO, mice previously treated with METH (3 mg/kg/day over 5 consecutive days) (Figure 3). Repeated ANOVA analysis showed a significant difference between two groups (Time6Group, F= 3.456, p = 0.042). The METH-induced DA release in the nucleus accumbes of Srr-KO mice previously treated with METH was significantly lower than that of WT mice previously treated with METH (Figure 3). These findings suggest that an administration of METH (1 mg/kg) failed to induce DA release in the nucleus accumbens of Srr-KO mice previously treated with METH.

METH-induced rewarding effects

Mice that had only received METH spent significantly more time in the METH assigned compartment relative to the saline treatment compartment. The mice conditioned with saline did not show a preference for either compartment on the CPP test day. These data showed that a single pairing with METH (1 mg/kg, s.c.)-induced CPP when mice were tested 24 h after conditioning. Two-way ANOVA analysis revealed a significant drug treatment effect for the METH-induced CPP score [genotype: F (1,40) = 0.37, p = 0.55; drug treatment: F (1,40)= 23.11, p,0.001], with no genotype x drug treatment interaction (F(1,40) = 0.44, p =0.51). Student's t-test indicated that repeated administration of METH (1 mg/kg) significantly increased CPP scores in both WT and Srr-KO mice (WT: t= 3.71, p = 0.001; SrrKO: t= 3.07, p = 0.006) (Figure 4). The data indicated that METH treatment induced rewarding effects in both WT mice and Srr-KO mice.

Phosphorylation of ERK1/2

ERK, a component of the mitogen-activated protein kinase (MAPK) intracellular signaling pathway, interacts with both dopamine and NMDA receptors in the brain. It has been reported that the phosphorylation of ERK1/2 plays a role in behavioral sensitization, after repeated administration of psychostimulants [30,31]. This study examined whether phosphorylation levels of ERK1/2 in the striatum of Srr-KO mice differed from that of WT mice. Two-way ANOVA analysis revealed a significant effect for METH-induced phosphorylation of ERK1/2 between WT and Srr-KO mice [ERK1; genotype: F (1,20) = 0.07, p = 0.80; drug treatment: F (1,20) = 2.12, p= 0.16; interaction: F (1,20) =6.13, p = 0.02; ERK2; genotype: F (1,20) =0.16, p= 0.70; drug treatment: F (1,20) = 0.75, p = 0.40; interaction: F (1,20) =12.89, p = 0.002]. Student's t-test indicated that a single dose of METH (3 mg/kg) significantly increased the phosphorylation of ERK1/2 in the WT mice [ERK1; WT: t =2.61, p = 0.03; ERK2; WT:

treated WT group (Student's t-test).
doi:10.1371/journal.pone.0035494.g003

t = 3.41, p =0.006] (Figure 5). In contrast, a single dose of METH (3 mg/kg) did not increase phosphorylation of ERK1/2 in Srr-KO

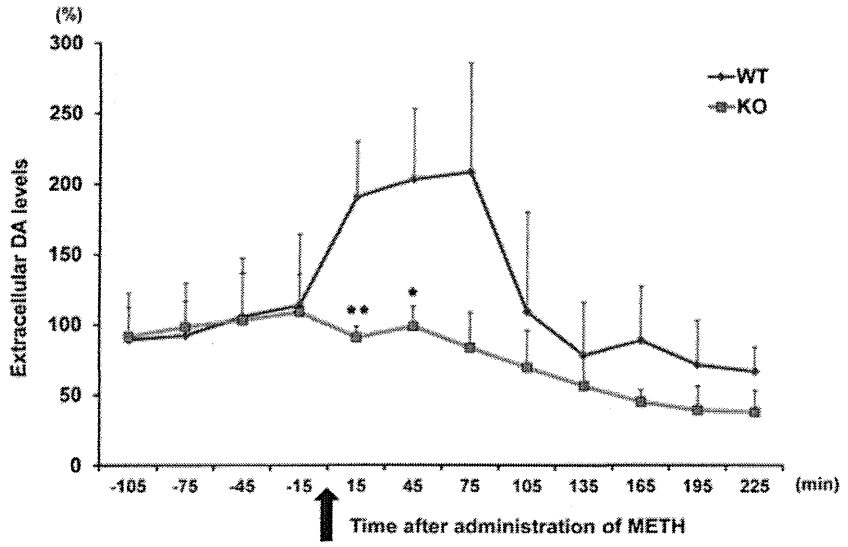

Figure 3. The effects of SRR on METH-induced increase of extracellular DA levels. A dose of METH (1.0 mg/kg, s.c) was injected into mice. The dialysate was collected in 30-min fractions, and DA levels were measured by HPLC. Basal extracellular DA levels in the nucleus accumbens were 3.84160.301 nmol/L (n = 12, mean 6 SEM). The values are the mean 6 SEM of 6 mice. *p,0.05, **p,0.01 as compared with the METH (1 mg/kg)

mice (ERK1; Srr-KO: t= 0.78, p= 0.46; ERK2; Srr-KO: t = 1.79, p= 0.10) (Figure 5).

In the hippocampus, two-way ANOVA analysis revealed no significant effect for METH-induced phosphorylation of ERK1/2 between WT and Srr-KO mice [ERK1; genotype: F (1,20) = 0.42, p = 0.53; drug treatment: F (1,20) = 0.23, p = 0.64; interaction: F (1,20) = 2.54, p= 0.13; ERK2; genotype: F (1,20) =7.23, p = 0.01; drug treatment: F (1,20)= 1.61, p = 0.21; interaction: F (1,20) = 0.41, p =0.53](Figure S3). In the frontal cortex, the phosphorylation of ERK1/2 was not detected between WT and Srr-KO mice (data not shown).

Discussion

The major findings of this study are that repeated administration of METH (3 mg/kg/day for 5 days) induced behavioral

Figure 4. METH-induced conditioned place preference (CPP) in mice. On days 4, 6, and 8, mice were treated with vehicle (10 ml/kg) or METH (1 mg/kg), and then confined in either a transparent or black compartment for 30 min. On days 5, 7, and 9, mice were given saline and placed in the non- METH

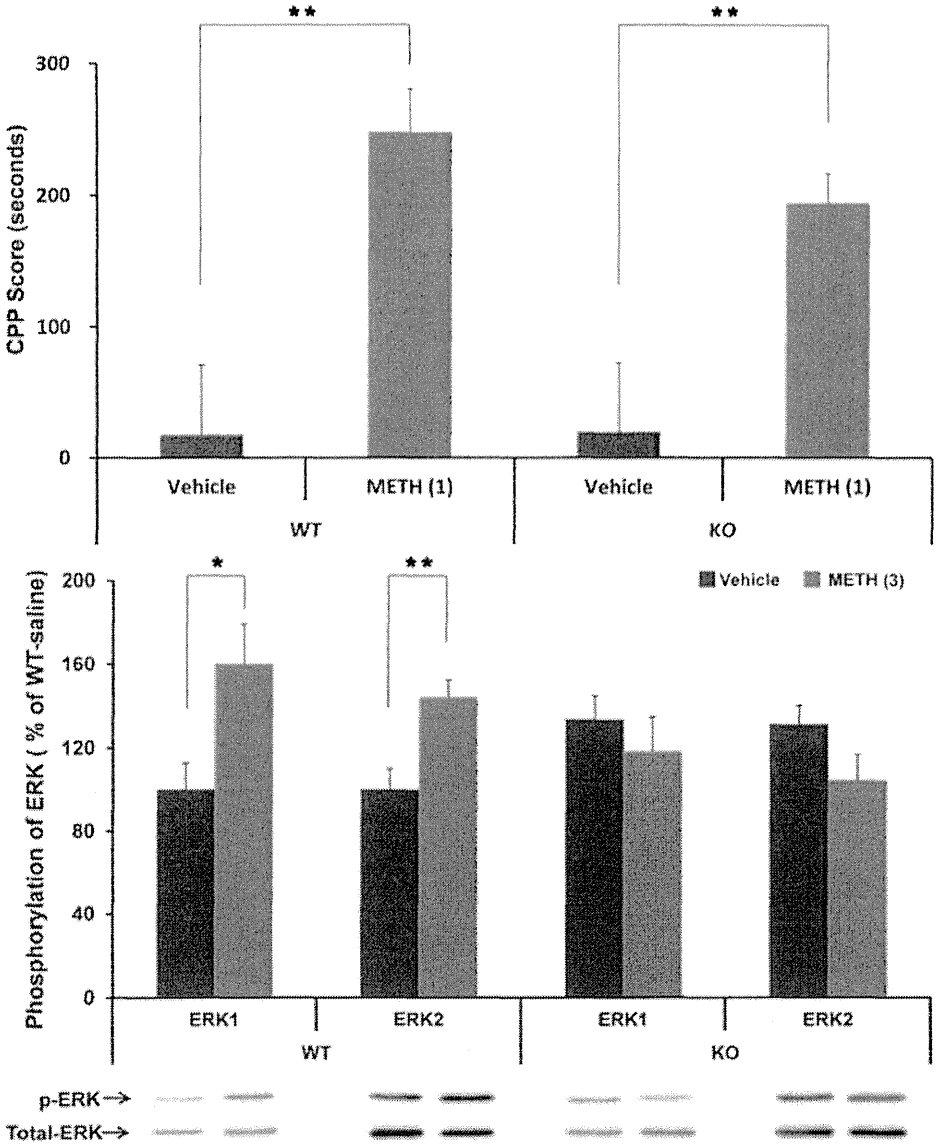

assigned compartment for 30 min. On day 10, the postconditioning test was performed as described in the Methods and Materials. Each value is the mean 6 SEM (n = 11 per group). **p,0.01 as compared with the vehicle treated group (Student's t-test).

doi:10.1371/journal.pone.0035494.g004

Figure 5. Phosphorylation of ERK1/2 in the striatum after a single dose of METH. Mice were sacrificed 15 minutes after a single dose of either METH (3 mg/kg, s.c.) or vehicle (10 ml/kg, s.c.). Western blot analysis of phospho-ERK1/2 and total ERK1/2 protein was performed as described in the Methods and Materials. Values are the mean 6 S.E.M. (n = 6 per group). *p,0.05, **p,0.01 as compared with the vehicle treated group (Student's t-test). doi:10.1371/journal.pone.0035494.g005

sensitization in WT mice, but not Srr-KO mice, and that a single dose of METH (3 mg/kg) produced the same changes in acute hyperlocomotion between Srr-KO and WT mice. From in vivo microdialysis, we found that METH-induced DA release in the nucleus accumbens of Srr-KO mice previously treated with METH (3 mg/kg/day over 5 consecutive days) was significantly attenuated as compared with WT mice previously treated with METH (3 mg/kg/day over 5 consecutive days). To our knowledge, this is the first report demonstrating the role of SRR in the development of METH-induced behavioral sensitization. Previously, we reported that levels of D-serine in the forebrain of Srr-KO mice were reduced to approximately 10–20% of those found in WT mice [27,29]. However, pretreatment with D-serine (900 mg/kg) did not alter hyperlocomotion in WT and Srr-KO mice after a single dose of METH (3 mg/kg), suggesting that decreased levels of D-serine in the brain do not affect METHinduced, acute hyperlocomotion in mice. Furthermore, pretreatment with D-serine (900 mg/kg/day) prior to each METH injection, failed to induce behavioral sensitization in Srr-KO mice. It is therefore unlikely that pretreatment with D-serine affects METH-induced behavioral abnormalities in either WT or Srr-KO mice. These findings suggest that SRR plays an important role in the development of behavioral sensitization in mice, following repeated METH administration.

Behavioral sensitization following the repeated administration of psychostimulants, including METH, is one manifestation of sensitization in the brain. The initiation of behavioral sensitization to psychostimulants is operationally defined as the transient

sequence of cellular and molecular events precipitated by repeated administration of psychostimulants that leads to the enduring changes in neural function responsible for behavioral augmentation [14,15,32,33]. The increase in extracellular DA is augmented in the nucleus accumbens and striatum following the repeated administration of psychostimulants. Together, the enhanced release of DA in the nucleus accumbens plays a role in the augmentation of behavior in the sensitized animals [14,15,32,33]. In this study, we found that Srr-KO mice pretreated with METH did not show the release of DA in the nucleus accumbens and behavioral augmentation after a challenge of METH, indicating a role of Srr in the development of behavioral sensitization after repeated administration of METH.

Accumulating evidence suggests that intracellular signaling pathways, including that of ERK1/2 play contributes greatly to the molecular pathophysiology of drug addiction [34–38]. Abused drugs including amphetamine and cocaine has been shown to activate ERK in a subset of medium-sized spiny neurons of the dorsal striatum and nucleus accumbens, through the combined action of NMDA and DA D_1 receptors [39–41]. Pretreatment with SL327 (30 mg/kg), a selective brain-penetrating inhibitor of MAP-kinase/ERK kinase, blocks the development of behavioral sensitization after repeated amphetamine treatment [39], suggesting a role for this pathway in long-lasting behavioral sensitization by psychostimulants. It has also been shown that phosphorylation of ERK1/2 in the striatum increases after administration of psychostimulants [30,31,40–41]. In this study, a single dose of METH (3 mg/kg) significantly increased the phosphorylation of ERK1/2 in the striatum of WT, but not SrrKO mice. This suggests that phosphorylation of ERK1/2 in the striatum following a single dose of METH, is at least in part, mediated by SRR, although the precise mechanisms are currently unclear. Previously, we reported that NMDA-induced neurotoxicity is significantly attenuated in the brains of Srr-KO mice, suggesting that D-serine controls the extent of NMDA receptormediated neurotoxic insults [27]. It is likely that the lack of behavioral sensitization seen in Srr-KO mice may be the result of decreased DA release and ERK1/2 phosphorylation, due to NMDA receptor hypofunction, although this will need to be investigated further.

The CPP paradigm is a widely used animal model on the rewarding effects of drugs [42]. The NMDA receptor antagonist MK-801 fails to block amphetamine-induced place preference in rats, suggesting that NMDA receptors may not be involved in the rewarding effects of psychostimulants [43]. Miyamoto et al. [44] reported that mice with mutant GluN2A, one of four GluN2 subunits (GluN2A-D) of the NMDA receptor, developed METHinduced place preference to the same degree as WT mice, whereas behavioral sensitization was significantly reduced in these mutants compared with WT mice. This suggests that the GluN2A subunit may play a role in the development of behavioral sensitization, but not rewarding effects, in mice repeated exposure to METH. In this study, Srr-KO mice developed METH-induced place preference to the same degree as WT mice. It is therefore unlikely that NMDA receptors play a major role in the development of METH-induced rewarding effects in mice.

Along with D-serine, glycine is also a co-agonist at the glycine modulatory site of the NMDA receptor [21]. We reported that brain derived levels of glycine and other amino acids, including, glutamate and glutamine, were comparable between WT and SrrKO mice [27,29], suggesting that glycine may not compensate for decreased D-serine levels in the brains of Srr-KO mice. In addition, forebrain levels of the NMDA subunits, GluN2A, GluN2B, and GluN1 were comparable between WT and SrrKO mice [27]. No difference was found in [^{3}H](+)-MK-801 binding between brain regions (frontal cortex, hippocampus, striatum, cerebellum) from WT and Srr-KO mice (Table S1). It would seem that the expression of NMDA receptors is comparable between WT and Srr-KO mice. It is highly probable that the reduced D-serine in the forebrain of Srr-KO mice may, in part, contribute to the lack of METH-induced behavioral sensitization, although this too needs to be examined in further studies.

In conclusion, this study has pointed to a role for SRR in the development of behavioral sensitization, but not rewarding effects, in mice that have been repeatedly exposed to METH. It also suggests that decreased DA release in the nucleus accumbens and decreased phosphorylation of the ERK1/2 protein may contribute to the lack of METH-induced behavioral sensitization in Srr-KO mice.

Materials and Methods

Animals

Srr-KO mice were generated from C57BL/6- derived embryonic stem cells transfected with a gene-targeting vector containing C57BL/6 mouse genomic DNA, and the colony was expanded by crossing with C57BL/6 mice [26]. The generation and genotyping of Srr-KO and WT mice with a pure C57BL/6 genetic background has been reported previously [26]. WT and Srr-KO mice aged 2–3 months were used for all behavioral studies. The mice were housed in clear polycarbonate cages (22.5633.8614.0 cm) in groups of 5 or 6 per cage, under a controlled 12/12-h light–dark cycle (lights on from 7:00 AM to 7:00 PM), with a room temperature of 2361uC and humidity at 5565%. The mice were given free access to water and food pellets. The experimental procedure (Permit Number: #23-151) was approved by the Animal Care and Use Committee of Chiba
University.

Drug Administration

METH (D-methamphetamine hydrochloride) was purchased from Dainippon-Sumitomo Pharmaceutical Ltd., (Osaka, Japan) and D-serine from Sigma-Aldrich Corporation (St. Louis, MO). METH was dissolved in physiological saline and injected subcutaneously (s.c.). The dose of METH was expressed as a hydrochloride salt. D-Serine dissolved in saline was administered orally at a concentration of 900 mg/kg of body weight. Other chemicals were purchased from commercial sources.

METH-induced Acute Hyperlocomotion

METH (1 and 3 mg/kg) or a vehicle of physiological saline (10 ml/kg) was administered s.c. into mice. Locomotor activity was measured using an animal movement analysis system (SCANET SV-10, Melquest, Toyama, Japan), as reported previously [45–47]. The system consisted of a rectangular enclosure (4806300 mm). The side walls (height, 60 mm) of the enclosure were equipped with 144 pairs of photosensors located 30 mm from the bottom edge and at 5 mm intervals. Recordings were taken from single animals. A pair of photosensors was scanned every 0.1 s to detect the animal movement. The intersection of paired photosensors (10 mm apart) in the enclosure was counted as one unit of locomotor activity. Data was collected for 180 min (60 min of habituation and for 120 min after the injection of METH or saline). To examine the role of D-serine in METH-induced acute hyperlocomotion, animals were pretreated with D-serine, before administration of METH. Thirty

minutes after a single oral dose of D-serine (900 mg/kg) or vehicle (10 ml/ kg), mice were administered a dose of METH (3 mg/kg, s.c). Locomotor activity was measured using the animal movement analysis system (SCANET SV-10, Melquest, Toyama, Japan), described above.

METH-induced Behavioral Sensitization

Wild type and Srr-KO mice were given a single s.c. dose of vehicle (10 ml/kg) or METH (3 mg/kg), and returned to their home cages. This process was repeated for each animal, over 5 consecutive days. One week after the final treatment, each mouse was given a low dose of METH (1 mg/kg, s.c.), and behavioral changes (locomotion) were measured using the animal movement analysis system (SCANET SV-10, Melquest, Toyama, Japan), described above.

Next, mice were pretreated with D-serine in order to examine its role in METH-induced behavioral sensitization. Both WT and Srr-KO mice were treated with either: vehicle (10 ml/kg) + METH (3 mg/kg) group or D-serine (900 mg/kg) + METH (3 mg/kg) group. Injections were given 30 min apart. After the administration of METH, mice were returned to their home cages and this treatment was repeated over 5 consecutive days. One week after the final treatment, all mice were given a low dose of METH (1 mg/kg, s.c.), and behavioral changes (locomotion) were measured using the animal movement analysis system (SCANET SV-10, Melquest, Toyama, Japan), described above.

Measurement of extracellular DA levels using in vivo microdialysis

Mice were anesthetized with sodium pentobarbital prior to the stereotaxic implantation of a probe into the nucleus accumbens (+1.1 mm anteroposterior, +1.0 mm mediolateral from the bregma, and 24.0 mm dorsoventral from the dura), according to the Franklin and Paxinos Atlas [48], as reported previously [49]. Probes were secured onto the skull using stainless-steel screws and dental acrylic. Twenty-four hours after surgery, in vivo microdialysis was performed on conscious and free moving mice. Probes were perfused continuously with artificial CSF (147 mM NaCl, 4 mM KCl, and 2.3 mM $CaCl_2$) at a rate of 2 ml/min. METH (1 mg/kg, s.c.) was administered into mice. The dialysate was collected in 30-min fractions. After in vivo microdialysis experiments, the position of probe in the nucleus accumbens was confirmed in all mice. The DA levels in each fraction were measured by high performance liquid chromatography (HPLC), with electrochemical detection using a reversed phase column (EICOMPAK PP-ODS, 4.6630 mm, Eicom, Kyoto, Japan) and a mobile phase 1% MeOH/100 mM phosphate buffer (pH 6.0) including 50 mg/L disodium EDTA disodium and 500 mg/L sodium decane-1-sulfonate.

Conditioned Place Preference (CPP)

The place conditioning paradigm (CPP; Brain Science Idea Inc., Osaka, Japan) was used to study METH-induced rewarding effects, as reported previously [49]. Mice were allowed to move freely between transparent and black compartments for 15 min, once a day, for 3 days (days 1–3), as preconditioning. On day 3, the time spent in each compartment was measured. There was no significant difference between time spent in the black compartment with a smooth floor and the time spent in the transparent compartment with a textured floor, indicating that mice had no compartment preference before conditioning. On days 4, 6, and 8, mice were administered either vehicle (10 ml/kg, s.c.) or METH (1.0 mg/kg, s.c.), and then confined in either the transparent or black compartment for 30 min. On days 5, 7, and 9, the mice were given vehicle and placed in the non- METH assigned compartment, for 30 min. On day 10, the post-conditioning test was performed without drug treatment, and the time individual mice spent in each compartment was measured for 15 min. A counterbalanced protocol was used in order to nullify the initial preference of each mouse. The CPP score was designated as the time spent in the drug-conditioning sites minus the time spent in the saline-conditioning sites.

Western Blot Analysis

In a preliminary experiment, we examined the time course for phosphorylation of ERK1/2 in the striatum, after a single dose of METH (3 mg/kg). We found increased phosphorylation of ERK1/2 15 min after a single METH administration (data not shown), consistent with a previous result [50]. In further experiments, mice were therefore sacrificed 15 min after dosing with either saline (10 ml/kg) or METH (3 mg/kg), then, the striatum, frontal cortex and hippocampus were dissected out on ice. Briefly, striatum from individual mice were frozen and homogenized in 500 ml of lysis buffer (20 mM TBS, pH 7.6, 10 mM NaF, 1 mM Na_3VO_4, 1% Triton x-100, 5 mM EDTA, 5 mM EGTA containing protease inhibitor) using a Polytron homogenizer. The sample was left to stand on ice for 30 min and then centrifuged at 10,0006g and 4uC for 30 min. Total protein in the supernatant was measured using the DC protein assay (BioRad, Hercules, CA). The sample was then diluted with 56 SDS sample buffer (62.5 mM Tris-HCl, pH 6.8, 10% glycerol, 2% SDS, 5% b-mercaptoethanol and bromophenol blue). Aliquots (10 mg protein) of protein were incubated for 5 min at 95uC, then separated using SDS-PAGE on 12% polyacrylamide gels. Proteins were transferred for 1 h onto a polyvinylidene difluoride (PVDF) membrane (GE Healthcare Amersham Hybond™-P, UK), using Trans Blot Mini Cell apparatus (Bio-Rad, Hercules, CA). The transfer buffer consisted of 25 mM Tris and 192 mM glycine. After protein transfer, membranes were blocked for 45 min in TBS-T (20 mM Tris-HCl, pH 7.6, 137 mM NaCl, 0.1% Tween20) containing 5% skimmed milk at RT, followed by incubation with anti-rabbit P44/42-ERK antibody (1:1000, Cell Signaling, Cambridge, MA), overnight at 4uC in TBS-T, containing 5% BSA. After three washes in TBS-T, membranes were incubated with secondary antibody (1:15,000) in TBS-T for 1 h at RT. After repeated washes, protein bands were detected using the ECL chemiluminescence detection system (GE Healthcare Bioscience, UK). Images were captured using a Fuji LAS3000-mini imaging system (Fujifilm, Tokyo, Japan), and chemiluminescence bands were quantified. To calculate the amount of phosphorylated protein relative to total protein, membranes were stripped in buffer (100 mM 2-mercaptoethanol, 2% SDS, and 62.5 mM TrisHCl, pH 6.7) at 60uC for 30 min, washed, blocked, re-incubated with rabbit anti-ERK (1:1000, Cell signaling, Cambridge, MA), and detected as described above.

Statistical Analysis

All data were expressed as a mean 6 standard error of the mean (S.E.M.). The behavior data, CPP score and ERK expression data were analyzed by two-way ANOVA (genotype vs. drug treatment). Student's t-test and one-way analysis of variance (ANOVA), followed Bonferroni/Dunn test were used for comparison between the two groups and comparison of multiple groups, respectively. The results of extracellular DA levels were analyzed by repeated one-way ANOVA, followed by the student's t-test. Values of $p<0.05$ were regarded as statistically significant.

Supporting Information

Figure S1 Effect of pretreatment with D-serine on acute hyperlocomotion after a single dose of METH. Thirty minutes after a single oral dose of vehicle (10 ml/kg) or D-serine (900 mg/kg), WT and Srr-KO mice were given a dose of METH (3 mg/kg, s.c.). Behavioral evaluation of locomotion was performed 2 hours after the dose of METH, as described in the Methods and Materials section. Each value is the mean 6 SEM (n= 7 per group). NS: Not significant (Student's t-test). (TIFF)

Figure S2 Effects of pretreatment with D-serine on behavioral sensitization after repeated administration of METH. Thirty minutes after a single oral administration of vehicle (10 ml/kg) or D-serine (900 mg/kg), WT and Srr-KO mice were dosed with METH (3 mg/kg) for 5 consecutive days. Seven days after the final dose of METH, a lower dose of METH (1 mg/kg, s.c.) was administered to all mice. Behavioral evaluation of locomotion was performed. Each value is the mean 6 SEM (n= 7 per group). ***p,0.01 as compared with the vehicle treated group (Bonferroni/Dunn method). NS: Not significant (Student's t-test). (TIFF)

Figure S3 Phosphorylation of ERK1/2 in the hippocampus after a single dose of METH. Mice were sacrificed 15 minutes after a single dose of either METH (3 mg/kg, s.c.) or vehicle (10 ml/kg, s.c.). Western blot analysis of phospho-ERK1/2 and total ERK1/2 protein was performed as described in the Methods and Materials. Values are the mean 6 S.E.M. (n= 6 per group). (TIFF)

Table S1 [^{3}H](+)-MK-801 binding to mouse brain regions. Binding of [^{3}H](+)-MK-801 (3 nM; 1.02 TBq/mmol, PerkinElmer, MA, USA) to the crude membranes from brain regions (frontal cortex, hippocampus, striatum, cerebellum) was performed. Non-specific binding was determined in the presence of 10 mM of (+)-MK-801. There were no differences between WT mice and Srr-KO mice. Values are the mean 6 S.E.M. (n= 7 per group). (DOCX)

Acknowledgments

Mao Horio was supported by Ishidsu Shun Memorial Scholarship, Japan. We would like to thank Professor Masaomi Iyo (Department of Psychiatry, Chiba University Graduate School of Medicine) for his support.

Author Contributions

Conceived and designed the experiments: KH. Performed the experiments: MH MK YF TI. Analyzed the data: MH KH. Contributed reagents/materials/analysis tools: RI HM. Wrote the paper: MH KH.

References

1. Hashimoto K (2007) Chapter 1.New Research on methamphetamine abuse. In Toolaney GH, ed. Nova Science Publishers, Inc, New York. pp 1–51.
2. Gonzales R, Mooney L, Rawson RA (2010) The methamphetamine problem in the united states. Annu Rev Public Health 31: 385–398.
3. Sato M, Chen CC, Akiyama K, Otsuki S (1983) Acute exacerbation of paranoid psychotic state after long-term abstinence in patients with previous methamphetamine psychosis. Biol Psychiatry 18: 429–440.
4. Ujike H, Sato M (2004) Clinical features of sensitization to methamphetamine observed in patients with methamphetamine dependence and psychosis. Ann N Y Acad Sci 1025: 279–287.
5. Featherstone RE, Kapur S, Fletcher PJ (2007) The amphetamine-induced sensitized state as a model of schizophrenia. Prog Neuropsychopharmacol Biol Psychiatry 31: 1556–1571.
6. Chen H, Wu J, Zhang J, Hashimoto K (2010) Recent topics on pharmacotherapy for amphetamine-type stimulants abuse and dependence. Curr Drug Abuse Rev 3: 222–238.
7. Karila L, Weinstein A, Aubin HJ, Benyamina A, Reynaud M, et al. (2010) Pharmacological approaches to methamphetamine dependence: A focused review. Br J Clin Pharmacol 69: 578–592.
8. Cadet JL, Jayanthi S, Deng X (2003) Speed kills: Cellular and molecular bases of methamphetamine-induced nerve terminal degeneration and neuronal apoptosis. FASEB J 17: 1775–1788.
9. Tata DA, Yamamoto BK (2007) Interactions between methamphetamine and environmental stress: Role of oxidative stress, glutamate and mitochondrial dysfunction. Addiction 102(Suppl 1): 49–60.
10. Earle ML, Davies JA (1991) The effect of methamphetamine on the release of glutamate from striatal slices. J Neural Transm Gen Sect 86: 217–222.
11. O'Dell SJ, Weihmuller FB, Marshall JF (1991) Multiple methamphetamine injections induce marked increases in extracellular striatal dopamine which correlate with subsequent neurotoxicity. Brain Res 564: 256–260.
12. Segal DS, Kuczenski R (1997) Repeated binge exposures to amphetamine and methamphetamine: Behavioral and neurochemical characterization. J Pharmacol Exp Ther 282: 561–573.
13. Chen JC, Liang KW, Huang YK, Liang CS, Chiang YC (2001) Significance of glutamate and dopamine neurons in the ventral pallidum in the expression of behavioral sensitization to amphetamine. Life Sci 68: 973–983.
14. Robinson TE, Becker JB (1986) Enduring changes in brain and behavior produced by chronic amphetamine administration: A review and evaluation of animal models of amphetamine psychosis. Brain Res 396: 157–198.
15. Pierce RC, Kalivas PW (1997) A circuitry model of the expression of behavioral sensitization to amphetamine-like psychostimulants. Brain Res Brain Res Rev 25: 192–216.
16. Karler R, Calder LD, Turkanis SA (1991) DNQX blockade of amphetamine behavioral sensitization. Brain Res 552: 295–300.
17. Wolf ME, Khansa MR (1991) Repeated administration of MK-801 produces sensitization to its own locomotor stimulant effects but blocks sensitization to amphetamine. Brain Res 562: 164–168.
18. Ohmori T, Abekawa T, Muraki A, Koyama T (1994) Competitive and noncompetitive NMDA antagonists block sensitization to methamphetamine. Pharmacol Biochem Behav 48: 587–591.
19. Kuribara H, Asami T, Ida I, Iijima Y, Tadokoro S (1992) Effects of repeated MK-801 on ambulation in mice and in sensitization following methamphetamine. Psychopharmacology (Berl) 108: 271–275.
20. Kim HS, Jang CG (1997) MK-801 inhibits methamphetamine-induced conditioned place preference and behavioral sensitization to apomorphine in mice. Brain Res Bull 44: 221–227.
21. Schell MJ (2004) The N-methyl D-aspartate receptor glycine site and D-serine metabolism: An evolutionary perspective. Philos Trans R Soc Lond B Biol Sci 359: 943–964.
22. Martineau M, Baux G, Mothet JP (2006) D-serine signalling in the brain: Friend and foe. Trends Neurosci 29: 481–491.
23. Wolosker H (2007) NMDA receptor regulation by D-serine: New findings and perspectives. Mol Neurobiol 36: 152–164.
24. Wolosker H, Blackshaw S, Snyder SH (1999) Serine racemase: A glial enzyme synthesizing D-serine to regulate glutamate-N-methyl-D-aspartate neurotransmission. Proc Natl Acad Sci U S A 96: 13409–13414.
25. Wolosker H, Sheth KN, Takahashi M, Mothet JP, Brady RO, Jr., et al. (1999) Purification of serine racemase: Biosynthesis of the neuromodulator D-serine. Proc Natl Acad Sci U S A 96: 721–725.
26. Miya K, Inoue R, Takata Y, Abe M, Natsume R, et al. (2008) Serine racemase is predominantly localized in neurons in mouse brain. J Comp Neurol 510: 641–654.
27. Inoue R, Hashimoto K, Harai T, Mori H (2008) NMDA- and beta-amyloid$_{1-42}$induced neurotoxicity is attenuated in serine racemase knock-out mice. J Neurosci 28: 14486–14491.
28. Basu AC, Tsai GE, Ma CL, Ehmsen JT, Mustafa AK, et al. (2009) Targeted disruption of serine racemase affects glutamatergic neurotransmission and behavior. Mol Psychiatry 14: 719–727.
29. Horio M, Kohno M, Fujita Y, Ishima T, Inoue R, et al. (2011) Levels of Dserine in the brain and peripheral organs of serine racemase (srr) knock-out mice. Neurochem Int 59: 853–859.
30. Rajadhyaksha A, Husson I, Satpute SS, Kuppenbender KD, Ren JQ, et al. (2004) L-type Ca^{2+} channels mediate adaptation of extracellular signal-regulated kinase 1/2 phosphorylation in the ventral tegmental area after chronic amphetamine treatment. J Neurosci 24: 7464–7476.
31. Valjent E, Pascoli V, Svenningsson P, Paul S, Enslen H, et al. (2005) Regulation of a protein phosphatase cascade allows convergent dopamine and glutamate signals to activate ERK in the striatum. Proc Natl Acad Sci U S A 102: 491–496.
32. Pierce RC, Kalivas PW (1997) A circuitry model of the expression of behavioral sensitization to amphetamine-like psychostimulants. Brain Res Rev 25: 192–216.
33. Vanderschuren LJMJ, Kalivas PW (2000) Alterations in dopaminergic and glutamatergic transmission in the induction and expression of behavioral sensitization: a critical review of preclinical studies. Psychopharmacology 151: 99–120.
34. Berke JD, Hyman SE (2000) Addiction, dopamine, and the molecular mechanisms of memory. Neuron 25: 515–532.

35. Chao J, Nestler EJ (2004) Molecular neurobiology of drug addiction. Annu Rev Med 55: 113–132.
36. Girault JA, Valjent E, Caboche J, Herve D (2007) ERK2: A logical AND gate critical for drug-induced plasticity? Curr Opin Pharmacol 7: 77–85.
37. Zhai H, Li Y, Wang X, Lu L (2008) Drug-induced alterations in the extracellular signal-regulated kinase (ERK) signalling pathway: Implications for reinforcement and reinstatement. Cell Mol Neurobiol 28: 157–172.
38. Mizoguchi H, Yamada K, Mizuno M, Mizuno T, Nitta A, et al. (2004) Regulations of methamphetamine reward by extracellular signal-regulated kinase 1/2/ets-like gene-1 signaling pathway via the activation of dopamine receptors. Mol Pharmacol 65: 1293–1301.
39. Valjent E, Corvol JC, Trzaskos JM, Girault JA, Herve D (2006) Role of the ERK pathway in psychostimulant-induced locomotor sensitization. BMC Neurosci 7: 20.
40. Gerfen CR, Paletzki R, Worley P (2008) Differences between dorsal and ventral striatum in Drd1a dopamine receptor coupling of dopamine- and cAMPregulated phosphoprotein-32 to activation of extracellular signal-regulated kinase. J Neurosci 28: 7113–7120.
41. Bertran-Gonzalez J, Bosch C, Maroteaux M, Matamales M, Herve D, et al. (2008) Opposing patterns of signaling activation in dopamine D_1 and D_2 receptor-expressing striatal neurons in response to cocaine and haloperidol. J Neurosci 28: 5671–5685.
42. Tzschentke TM (1998) Measuring reward with the conditioned place preference paradigm: A comprehensive review of drug effects, recent progress and new issues. Prog Neurobiol 56: 613–672.
43. Hoffman DC (1994) The noncompetitive NMDA antagonist MK-801 fails to block amphetamine-induced place conditioning in rats. Pharmacol Biochem Behav 47: 907–912.
44. Miyamoto Y, Yamada K, Nagai T, Mori H, Mishina M, et al. (2004) Behavioural adaptations to addictive drugs in mice lacking the NMDA receptor epsilon1 subunit. Eur J Neurosci 19: 151–158.
45. Zhang L, Kitaichi K, Fujimoto Y, Nakayama H, Shimizu E, et al. (2006) Protective effects of minocycline on behavioral changes and neurotoxicity in mice after administration of methamphetamine. Prog Neuropsychopharmacol Biol Psychiatry 30: 1381–1393.
46. Hagiwara H, Iyo M, Hashimoto K (2009) Mithramycin protects against dopaminergic neurotoxicity in the mouse brain after administration of methamphetamine. Brain Res 1301: 189–196.
47. Chen H, Wu J, Zhang J, Fujita Y, Ishima T, et al. (2012) Protective effects of the antioxidant sulforaphane on behavioral changes and neurotoxicity in mice after the administration of methamphetamine. Psychopharmacologyin press.
48. Franklin KBL, Paxinos G (1997) The mouse brain in stereotaxic coordinates. San Diego, CA: Academic Press.
49. Fujita Y, Kunitachi S, Iyo M, Hashimoto K (2012) The antibiotic minocycline prevents methamphetamine-induced rewarding effects in mice. Pharmacol Biochem Behav 101: 303–306.
50. Shi X, McGinty JF (2007) Repeated amphetamine treatment increases phosphorylation of extracellular signal-regulated kinase, protein kinase B, and cyclase response element-binding protein in the rat striatum. J Neurochem 103: 706–713.

Astrocyte-induced cortical vasodilation is mediated by D-serine and endothelial nitric oxide synthase

Jillian L. LeMaistre Stobart[a,b,1], Lingling Lu[a,b,1], Hope D. I. Anderson[c,d], Hisashi Mori[e], and Christopher M. Anderson[a,b,2]

[a]Department of Pharmacology and Therapeutics, University of Manitoba, Winnipeg, MB, Canada R3E 0T6; [b]Division of Neurodegenerative Disorders, St. Boniface Hospital Research, Winnipeg, MB, Canada R2H 2A6; [c]Faculty of Pharmacy, University of Manitoba, Winnipeg, MB, Canada R3E 0T5; [d]Canadian Centre for Agri-Food Research in Health and Medicine, St. Boniface Hospital Research, Winnipeg, MB, Canada R2H 2A6; and [e]Department of Molecular Neuroscience, Graduate School of Medicine and Pharmaceutical Sciences, University of Toyama, Toyama 930-0194, Japan

Edited by Solomon H. Snyder, The Johns Hopkins University School of Medicine, Baltimore, MD, and approved January 11, 2013 (received for review September 14, 2012)

Astrocytes play a critical role in neurovascular coupling by providing a physical linkage from synapses to arterioles and releasing vaso-active gliotransmitters. We identified a gliotransmitter pathway by which astrocytes influence arteriole lumen diameter. Astrocytes synthesize and release NMDA receptor coagonist, D-serine, in response to neurotransmitter input. Mouse cortical slice astrocyte activation by metabotropic glutamate receptors or photolysis of caged Ca^{2+} produced dilation of penetrating arterioles in a manner attenuated by scavenging D-serine with D-amino acid oxidase, deleting the enzyme responsible for D-serine synthesis (serine racemase) or blocking NMDA receptor glycine coagonist sites with 5,7-dichlorokynurenic acid. We also found that dilatory responses were dramatically reduced by inhibition or elimination of endothelial nitric oxide synthase and that the vasodilatory effect of endothelial nitric oxide synthase is likely mediated by suppressing levels of the vasoconstrictor arachidonic acid metabolite, 20-hydroxy arachidonic acid. Our results provide evidence that D-serine coactivation of NMDA receptors and endothelial nitric oxide synthase is involved in astrocyte-mediated neurovascular coupling.

two-photon | functional hyperemia | Ca^{2+} uncaging

Cerebral blood flow is regulated by autoregulation, which maintains constant flow during changes in systemic blood pressure, and functional hyperemia, which refers to matched increases in blood flow to brain areas with high neuronal energy demand. Intracerebral arterioles and capillaries account for 30–40% of total cerebrovascular blood flow resistance (1), and therefore, changes to the diameter of small penetrating cortical vessels result in significant changes in local cerebral blood flow. Astrocytes have endfeet directly apposed to these resistance vessels and are critical regulators of arteriole lumen diameter. Astrocyte endfeet express Ca^{2+}-activated K^+ channels that gate vasodilatory K^+ efflux in response to glutamatergic input (2, 3). Glutamate neurotransmission also causes Ca^{2+}-dependent arachidonic acid (AA) metabolism and release of vasodilatory AA metabolites from astrocytes, including prostaglandin E_2 (PGE_2), produced by cyclooxygenase (COX), and epoxyeicosatrienoic acids (EETs), produced by cytochrome P450 epoxygenase (4–8). Astrocyte-derived AA can also be metabolized by cytochrome P450 ω-hydroxylase to the vasoconstrictor, 20-hydroxyeicosatetranoic acid (20-HETE) (4, 6–8). Ambient tissue oxygen levels dictate whether astrocytes produce AA-dependent vasodilation or vasoconstriction in brain slices and isolated retina (6, 7). Production of 20-HETE is preferred at high pO_2 (95% O_2 in solution) (6–8), whereas pO_2 closer to physiologic levels (20% O_2) inhibits prostaglandin-lactate transporter activity, producing high extracellular PGE_2 levels (7) and reduced 20-HETE synthesis (6).

Application of glutamate or NMDA directly to the brain surface dilates pial arteries (9, 10) by a mechanism mediated by NMDA receptors (9–12) and neuronal nitric oxide synthase (nNOS) (13–15). Although NO is capable of increasing lumen diameter by directly affecting smooth muscle, it may also trigger vasodilation at physiologic pO_2 by reducing ω-hydroxylase activity and 20-HETE production, thereby shifting the balance of constrictor and dilator AA metabolites derived from astrocytes (4, 16, 17). In vivo, it was suggested NO derived from nNOS, specifically, reduces 20-HETE levels (17), but there is no further evidence of a specific link between nNOS and astrocyte AA metabolism in neurovascular coupling. Endothelial NOS (eNOS) plays a role in baseline brain vascular tone and pathological hyperemia (13, 18–21), but there has not yet been a connection made between eNOS, astrocyte function, and hyperemic vasodilation.

NMDA receptors are activated by binding of glutamate and a coagonist that binds to a strychnine-insensitive glycine regulatory site (22). D-Serine is more effective than glycine as an NMDA receptor coagonist (23–25) and has a brain distribution that closely parallels that of NMDA receptors (26). In addition, D-serine is extensively distributed in glial cells (26, 27), is released as a gliotransmitter by Ca^{2+}-dependent exocytosis in response to glutamatergic input (28), and contributes to astrocyte–neuron communication (29–31). Given the established role of NMDA receptors in hyperemic blood flow regulation, we hypothesized that astrocyte D-serine is directly involved in regulating the lumen diameter of brain resistance vessels. We showed previously that isolated middle cerebral arteries dilated in response to exogenous glutamate and D-serine treatment by an NMDA receptor-mediated mechanism (32). The goal of the current study was to determine whether endogenous D-serine is involved in astrocyte-mediated neurovascular coupling in cortical penetrating arterioles. We demonstrated that endogenous D-serine contributes to the vasodilatory response produced by direct astrocyte activation. We also provide evidence that NMDA receptors and eNOS are involved in this response, identifying a signal linking astrocytes and eNOS-mediated vasodilation.

Results

Metabotropic Glutamate Receptor Activation Causes D-Serine–Mediated Dilation of Cortical Arterioles. Immunohistochemistry in fixed cortical slices revealed D-serine immunoreactivity in astrocyte endfeet apposed to penetrating arterioles (Fig. 1). D-Serine signal (Fig. 1*A*) was detected in cells coexpressing the astrocyte marker, GFAP (Fig. 1*B*), around arterioles labeled with isolectin B_4 (Fig. 1*C*). This suggests there is a D-serine pool in close proximity to cortical supply vessels. Separately, the metabotropic glutamate receptor (mGluR) agonist, (±)-1-aminocyclopentane-*trans*-

Author contributions: H.D.I.A. and C.M.A. designed research; J.L.S. and L.L. performed research; H.M. contributed new reagents/analytic tools; J.L.S., L.L., H.D.I.A., and C.M.A. analyzed data; and J.L.S. and L.L. wrote the paper.

The authors declare no conflict of interest.

This article is a PNAS Direct Submission.

[1]J.L.S. and L.L. contributed equally to this work.

[2]To whom correspondence should be addressed. E-mail: chris.anderson@med.umanitoba.ca.

This article contains supporting information online at www.pnas.org/lookup/suppl/doi:10.1073/pnas.1215929110/-/DCSupplemental.

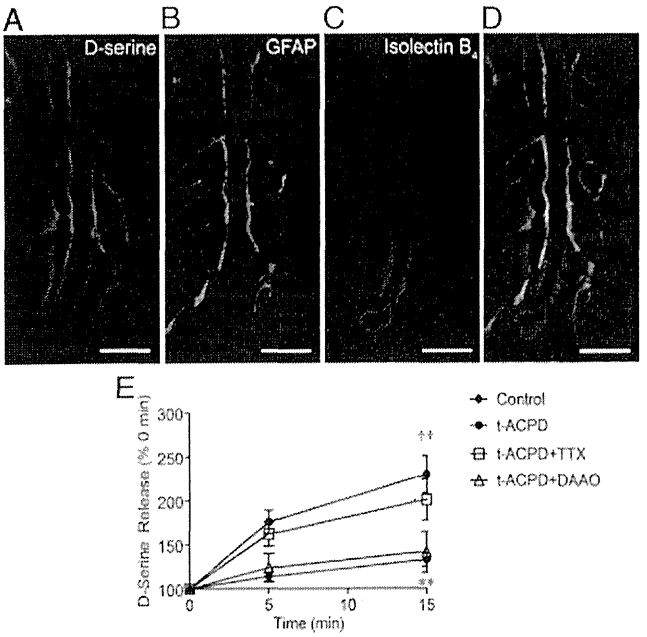

Fig. 1. D-serine localization to perivascular astrocyte endfeet in fixed cortical slices. (*A–D*) D-serine immunoreactivity (*A*, red) was localized to perivascular sites colabeled with the astrocyte marker, GFAP (*B*, green) in glutaraldehyde-fixed cortical slices (30 μm) from 14–19-d-old mice. Cerebrovasculature was labeled with isolectin B_4 (*C*, blue). (*D*), Overlay of *A–C* (scale bar, 20 μm). (*E*) mGluR agonist *t*ACPD (100 μM) induced significant release of D-serine from brain slices compared with untreated controls. Detection was eliminated by coexposure to DAAO (0.1 Units/mL). Data are mean ± SEM; $^{**}P < 0.0.01$ for *t*ACPD compared with control; †† $P < 0.01$ for *t*ACPD/TTX compared with control using two-way ANOVA with Bonferroni post hoc test.

1,3-dicarboxylic acid (*t*ACPD), has been shown to increase intracellular astrocyte Ca^{2+} levels and dilate local arterioles (7, 33), as well as stimulate D-serine release in a Ca^{2+} and SNARE-protein–dependent manner (28, 34). We confirmed that *t*ACPD treatment of acute cortical slices (100 μM) stimulated significant accumulation of extracellular D-serine after 15 min of exposure using a bulk chemiluminescence assay (Fig. 1*E*). Pretreatment with the D-serine catabolic enzyme, D-amino acid oxidase (DAAO), significantly reduced extracellular D-serine accumulation, indicating specific detection of D-serine. Tetrodotoxin (TTX) pretreatment had no effect, suggesting neuronal D-serine pools accessible by depolarization (35) are not involved in this response.

We exposed cortical slices to *t*ACPD and simultaneously monitored perivascular astrocyte Ca^{2+} and neighboring arteriole diameter in real time using two-photon laser scanning microscopy (Fig. 2 *A–C*). In slices maintained in artificial cerebrospinal fluid (aCSF) with 20% O_2, *t*ACPD enhanced rhodamine-2 fluorescence in astrocytes in a manner temporally associated with dilatory responses in cortical arterioles (Fig. 2*D*). *t*ACPD produced a maximal lumen diameter increase of 3.7 ± 0.1%, 75 s after exposure (Fig. 2*E*; maximal of 4.1 ± 0.8% without fixing the time point). Dilatory responses were assessed as area under the curve (AUC) between time 0 (*t*ACPD addition) and return to baseline (Fig. 2*E*). Preincubation of slices with DAAO (0.1 units/mL) significantly reduced vasodilation (Fig. 2*F*), whereas addition of exogenous D-serine to compete for DAAO activity restored vasodilatory responses. *t*ACPD-induced vasodilation in cortical slices isolated from mice lacking the D-serine synthesis enzyme, serine racemase (SR) was dramatically reduced, further indicating an important role for D-serine (Fig. 2*G*). These experiments demonstrate that perivascular astrocytes contain D-serine that can be released in quantities sufficient to increase arteriolar lumen diameter in glutamatergic neurotransmission simulated by mGluR activation. TTX pretreatment did not affect vasodilatory responses (Fig. 2*H*), arguing against an effect of D-serine derived from neuronal stores accessed by depolarization.

Direct Astrocyte Activation Causes D-Serine–Dependent Dilation of Cortical Arterioles. To directly link astrocyte Ca^{2+} elevations with vasodilatory responses, we stimulated increases in cytoplasmic Ca^{2+} levels of single rhodamine-2-labeled perivascular astrocytes using flash photolysis of the caged Ca^{2+} compound, o-nitrophenyl-EGTA AM (NP-EGTA; Fig. S1). Astrocyte Ca^{2+} (rhodamine-2) and arteriole diameter were subsequently monitored (Fig. 3 *A–C*). Astrocyte Ca^{2+} increases consistently correlated with dilation of neighboring cortical arterioles (Fig. 3*D*, representative experiment). Average vasodilation peaked at 5.7 ± 0.2%, 105 s after stimulation (Fig. 3*B*; 7.0 ± 0.9% without fixing the time point). DAAO significantly reduced vasodilation in a manner reversed by addition of exogenous D-serine after flash photolysis (Fig. 3*F*). Similarly, vasodilation was significantly inhibited by deletion of SR (Fig. 3*G*). These data demonstrate that endogenous D-serine plays a role in cortical vasodilation resulting from direct activation of a single perivascular astrocyte by Ca^{2+} uncaging. TTX (1 μM) did not significantly alter

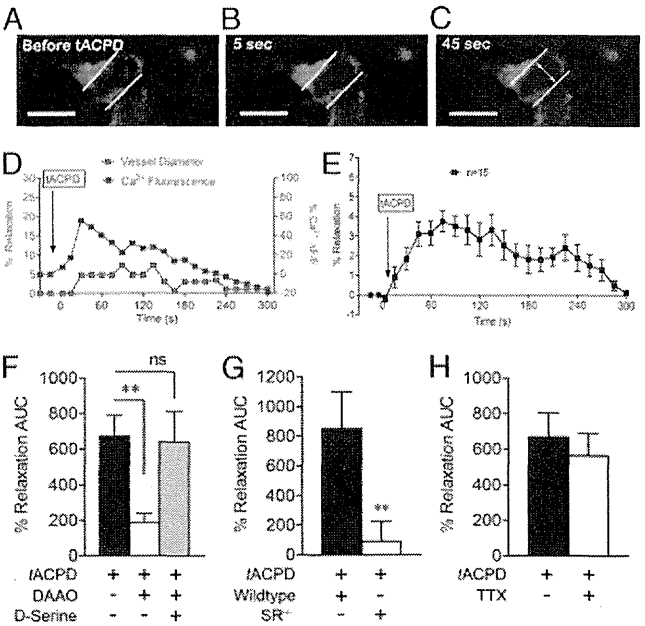

Fig. 2. *t*ACPD induces D-serine–dependent cortical vasodilation. Bath application of *t*ACPD (100 μM) elevated astrocyte Ca^{2+} (green, Rhod 2) and triggered arteriolar (red, isolectin B_4) vasodilation in a temporally correlated manner. (*A–C*) Representative images for a single astrocyte–arteriole pair before *t*ACPD addition (*A*) and 5 (*B*) and 45 (*C*) s after (scale bar, 15 μm). (*D*) Representative plot of changes in astrocyte Ca^{2+} (blue) and arteriole diameter (red) after *t*ACPD treatment. (*E*) Plot of average dilation of 15 vessels after *t*ACPD treatment over 300 s. Data are mean ± SEM. (*F*), DAAO significantly inhibited vasodilation of arterioles after *t*ACPD application, whereas exogenous D-serine (100 μM) with DAAO recovered the dilatory effect of *t*ACPD. (*G*) Genetic deletion of SR ($SR^{-/-}$) eliminated the vasodilatory response to *t*ACPD. (*H*) TTX did not affect *t*ACPD-induced vasodilation. For *G* and *H*, data are mean ± SEM of total AUC for individual plots of percent relaxation versus time. $^{**}P < 0.01$ using one-way ANOVA with Student Newman–Keuls test (>2 groups) or *t* tests (2 groups).

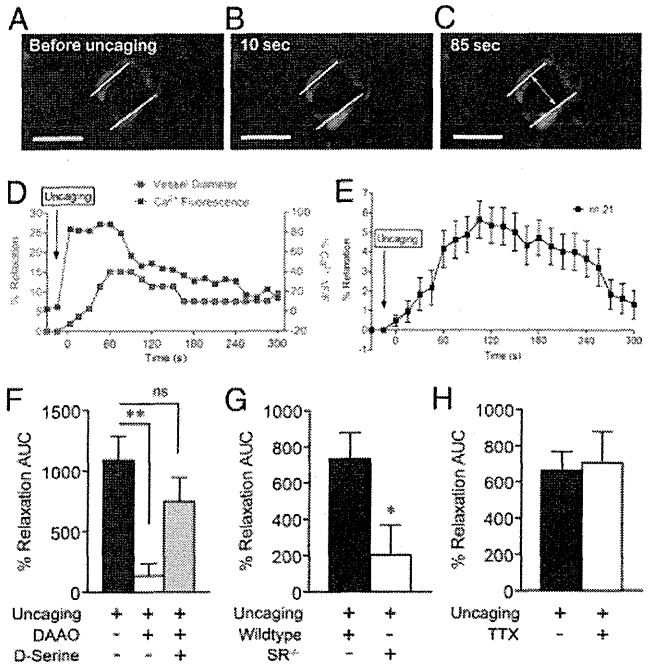

Fig. 3. Direct astrocyte Ca^{2+} uncaging leads to D-serine–dependent cortical vasodilation. Flash photolysis of o-nitrophenyl-EGTA in perivascular astrocyte endfeet stimulated elevation of local Ca^{2+} levels (green, Rhod 2) in a manner that temporally corresponded with an increase in lumen diameter of a neighboring arteriole (red, isolectin B_4). (*A–C*) Representative images of a single perivascular astrocyte and arteriole are shown before (*A*) and after (*B* and *C*) flash photolysis (scale bar, 15 μm). (*D*) Representative plot of changes in astrocyte Ca^{2+} (blue) and arteriole diameter (red) after photolysis. (*E*) Plot of average dilation of 21 vessels after astrocyte Ca^{2+} uncaging over 300 s. Data are mean ± SEM. (*F*) DAAO (0.1 Units/mL) significantly inhibited vasodilation induced by direct astrocyte activation, whereas exogenous D-serine (100 μM) with DAAO recovered the dilatory effect. (*G*) Genetic deletion of SR ($SR^{-/-}$) eliminated the vasodilatory response to astrocyte Ca^{2+} uncaging. (*H*) TTX (1 μM) did not affect vasodilation induced by astrocyte Ca^{2+} uncaging. For *G* and *H*, data are mean ± SEM of total AUC for individual plots of percent relaxation versus time. $*P < 0.05$, $**P < 0.01$ using one-way ANOVA with Student Newman–Keuls test (>2 groups) or *t* tests (2 groups).

vasodilatory responses (Fig. 3*H*), suggesting neuronal excitation is not necessary for direct astrocyte-mediated vasodilation.

D-Serine–Dependent Vasodilation Is Dependent on Glutamate Corelease and NMDA Receptors. Cortical slices were exposed to the NMDA receptor competitive glycine/D-serine coagonist site antagonist 5,7-dichlorokynurenic acid (DCKA; 100 μM) or the competitive glutamate-site antagonist 2-amino-5-phosphonopentanoate (AP5; 50 μM), before flash photolysis of caged Ca^{2+}. Both DCKA and AP5 significantly reduced vasodilatory responses (Fig. 4*A*). Preincubation of cortical slices with glutamate dehydrogenase (GDH; 1 U/mL) also attenuated arteriole dilation resulting from flash photolysis (Fig. 4*B*), indicating that both glutamate and D-serine (Figs. 2 and 3) are involved in astrocyte-mediated vasodilation. In agreement, *t*ACPD caused TTX-independent bulk release of endogenous glutamate from cortical slices (Fig. 4*C*), supporting the idea that glutamate and D-serine are coreleased from astrocytes and play a joint role in neurovascular coupling.

Astrocyte-Mediated Vasodilation Is Dependent on PGE_2 and eNOS. Our data demonstrate that intact endothelium and eNOS are required for D-serine and glutamate to increase lumen diameter in isolated middle cerebral arteries (32). We thus tested the hypothesis that D-serine and glutamate-induced vasodilation in cortical slice arterioles is mediated by eNOS. In response to astrocyte Ca^{2+} uncaging, genetic deletion of eNOS dramatically attenuated increases in lumen diameter compared with treatment controls (Fig. 5*A*). We also measured vasodilatory responses to an exogenous glutamate and D-serine mixture (10 μM each with 1 μM TTX) in the presence and absence of the eNOS inhibitor, N5-(1-iminoethyl)-L-ornithine (L-NIO; 3 μM). L-NIO significantly reduced arteriole dilation by glutamate and D-serine (Fig. 5*B*), directly linking D-serine with eNOS activity and vasodilation in cortical slices.

Several studies have demonstrated that astrocyte-induced cortical vasodilation is mediated by COX-dependent metabolism of AA to PGE_2 (5, 7, 33). We therefore tested for PGE_2 involvement in our model by using indomethacin (INM; 100 μM) to inhibit COX. INM alone reduced vasodilation produced by astrocyte Ca^{2+} uncaging by 87% (Fig. 5*C*). This is not significantly different from the L-NIO-mediated reduction (55%). Combined, INM and L-NIO significantly enhanced the effect of L-NIO alone, producing vasoconstriction in response to astrocyte Ca^{2+} uncaging (Fig. 5*C*). *t*ACPD-induced astrocyte activation increased PGE_2 levels in a manner independent of L-NIO or genetic eNOS elimination (Fig. 5*D*), indicating that eNOS does not cause vasodilation by directly influencing PGE_2.

eNOS Causes Vasodilation by Suppressing 20-HETE Production. There is substantial evidence that NO inhibits production of the vasoconstrictor AA metabolite 20-HETE (36), leading to vasodilation in brain microvasculature (4, 17), but any contribution of eNOS to this pathway is yet to be identified. In our hands, brain slice production of 20-HETE in the presence of *t*ACPD was significantly enhanced in eNOS-null cortical slices (Fig. 6*A*), demonstrating that eNOS activity suppresses 20-HETE production in this model. To determine whether suppression of 20-HETE participates in eNOS-mediated vasodilation, we examined the effect of eNOS inhibition by L-NIO in the absence of a functional 20-HETE production pathway, suppressed by the

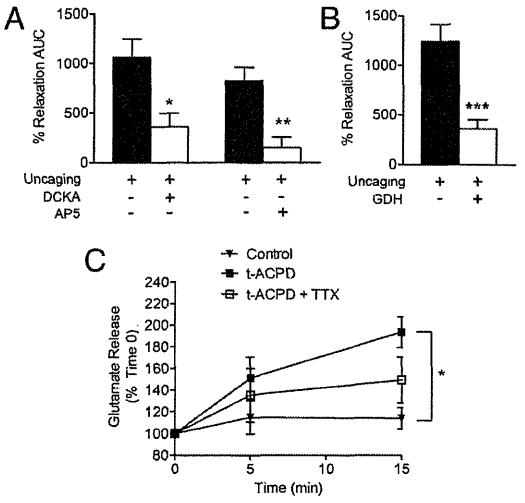

Fig. 4. Cortical vasodilation by D-serine is dependent on glutamate and NMDA receptors. (*A*) tACPD induced significant TTX-insensitive (1 μM) glutamate release, relative to control cortical slices ($*P < 0.05$ using two-way ANOVA with Bonferroni test). (*B*) GDH (1 U/mL) significantly reduced arteriole vasodilation induced by astrocyte Ca^{2+} uncaging ($***P < 0.001$, *t* test). (*C*) Competitive NMDA receptor antagonists DCKA (glycine site, 100 μM) and AP5 (glutamate site, 50 μM) significantly blocked arteriole vasodilation induced by direct astrocyte Ca^{2+} uncaging ($*P < 0.05$; $**P < 0.01$, one-way ANOVA with Student Newman–Keuls test). All data are mean ± SEM.

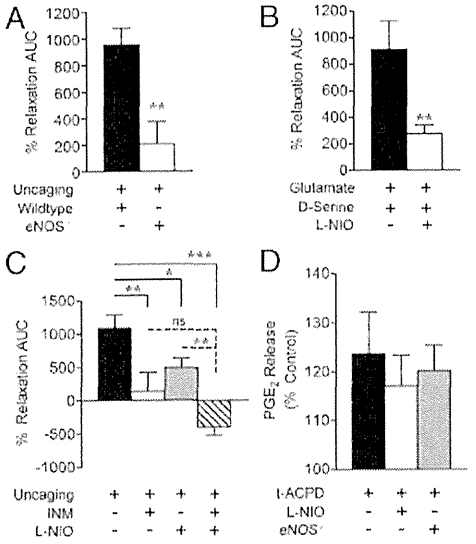

Fig. 5. Astrocyte-induced cortical vasodilation is mediated by PGE_2 and eNOS. (*A*) eNOS-null mice displayed reduced cortical vasodilatory efficacy in response to astrocyte Ca^{2+} uncaging compared with C57 wild-type mice (**$P <$ 0.01, *t* test). (*B*) Coapplication of glutamate (10 μM), D-serine (10 μM), and TTX (1 μM) produced cortical slice vasodilation sensitive to inhibition by the eNOS selective antagonist L-NIO (3 μM, **$P < 0.01$, *t* test). (*C*) Both the COX inhibitor INM (100 μM) and eNOS inhibitor L-NIO (3 μM) significantly reduced vasodilation in response to astrocyte Ca^{2+} uncaging. Combined INM and L-NIO caused significant vasoconstriction in response to astrocyte Ca^{2+} uncaging (*$P < 0.05$, **$P < 0.01$, ***$P < 0.001$ using one-way ANOVA with Student Newman–Keuls test). (*D*) PGE_2 release from cortical slices was measured by ELISA 5 min after *t*ACPD treatment and was not significantly affected by treatment with L-NIO (3 μM) or genetic eNOS deletion (ns, $P > 0.05$ using one-way ANOVA with Student Newman–Keuls test). All data are mean ± SEM.

CYP4A (ω-hydroxylase) inhibitor *N*-hydroxy-N'-(4-n-butyl-2-methylphenyl)formamidine (HET0016; 100 nM). Vasodilation induced by astrocyte Ca^{2+} uncaging was significantly inhibited by L-NIO alone but not in combination with HET0016 (Fig. 6*B*), suggesting that eNOS vasodilation is dependent on activity of the 20-HETE pathway.

Discussion

Here, we provided evidence that endogenous D-serine is a mediator of neurovascular coupling. D-Serine was responsible for astrocyte-induced dilation of penetrating cortical arterioles in a manner dependent on coavailability of extracellular glutamate and NMDA receptors. We also demonstrated that astrocyte-mediated cortical vasodilation is at least partially dependent on eNOS-derived suppression of 20-HETE.

Several lines of evidence support involvement of astrocyte D-serine in dilation of penetrating cortical arterioles in brain slices. D-Serine immunoreactivity was identified in perivascular astrocyte endfeet, in agreement with a previous report (26). Also consistent with published data (28), we found that simulating glutamatergic neurotransmission by exposing cortical slices to *t*ACPD caused significant efflux of D-serine into the bathing medium (28). These data together suggest there is a source of D-serine available for regulated release at the neurovascular unit. We then showed that DAAO and SR deletion significantly inhibited dilation of brain slice–penetrating cortical arterioles induced by *t*ACPD. This observation established a critical role for endogenous D-serine in regulating brain vascular lumen diameter, and this role is supported further by the demonstration that vasodilatory effects were mitigated by interfering with specific binding for D-serine in the NMDA receptor complex by DCKA. Because *t*ACPD activates both neuronal and astrocytic mGluRs, we considered the possibility that the vasodilatory effect of D-serine is independent of astrocyte activation by *t*ACPD. Although the failure of TTX to suppress D-serine release and cortical vasodilation argues against this idea, we more precisely ascertained the role of astrocytes in D-serine–mediated vasodilation by using flash photolysis of caged Ca^{2+} (NP-EGTA) in perivascular astrocyte endfeet. Direct astrocyte activation was sufficient to increase arteriolar lumen diameter in cortical slices. Moreover, uncaging-induced vasodilation was blocked by more than 88% by DAAO and 72% by SR deletion, providing further support for a vasodilatory pathway originating with glutamate neurotransmission and leading to astrocyte Ca^{2+} elevation, D-serine release from astrocytes, and vascular smooth muscle relaxation.

The impact of observed changes to the lumen diameter on blood flow is an important consideration. Poiseuille's Law dictates that resistance to blood flow decreases as a function of the fourth power of any increases in lumen diameter. Therefore, a 7% increase in lumen diameter (average achievement with uncaging) reduces resistance by a more impressive magnitude of 24%. In addition, comparisons across experimental conditions are critical because some models use preconstriction paradigms to achieve a much higher magnitude of vasodilation (33, 37). Our observations are consistent with vasodilation magnitudes observed by another group using brain slices maintained without preconstriction at equal aCSF oxygenation (7). These points, coupled with observations that vasodilation in vitro likely underestimates COX-mediated vasodilation seen in pressurized vessels in vivo (5), support speculation that our observed vasodilatory magnitudes in vitro translate into meaningful blood flow changes in vivo.

Our data support a vasodilatory mechanism of D-serine mediated by coactivation of NMDA receptors with glutamate. Again, cortical vasodilation induced by astrocyte Ca^{2+} uncaging was significantly attenuated by DCKA, directly indicating that activation of NMDA receptor glycine sites is involved. Importantly, this effect was also inhibited by AP5, indicating that occupation of the NMDA receptor glutamate binding site is also required for vasodilation in this paradigm. Paired involvement of glutamate and D-serine is further supported by our observations that *t*ACPD stimulated both glutamate and D-serine release (Figs. 4*C* and 1*E*, respectively) and that the presence of the glutamate catabolic enzyme GDH eliminated cortical vasodilation initiated by Ca^{2+} uncaging. Overall, these results show that both coagonists of NMDA receptors are required for a significant component of astrocyte-induced vasodilation in cortical slices. There is a report that AP5 does not affect cortical vasodilation in response to *t*ACPD (33). Although this is seemingly

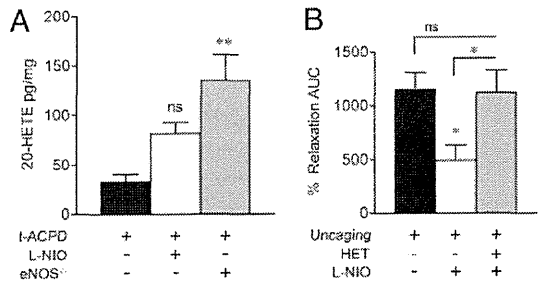

Fig. 6. eNOS inhibits 20-HETE production. (*A*) Cortical slice 20-HETE production in response to *t*ACPD was statistically unchanged by L-NIO (ns, $P >$ 0.05) and increased by eNOS deletion (**$P < 0.01$, one-way ANOVA with Student Newman–Keuls test). (*B*) Alone, L-NIO (3 μM) significantly reduced cortical vasodilation induced by astrocyte Ca^{2+} uncaging (*$P < 0.05$, one-way ANOVA with Student Newman–Keuls test). This effect was lost in the presence of HET0016 (HET, 100 nM; ns, $P > 0.05$), which interferes with 20-HETE formation. All data are mean ± SEM.

inconsistent with our results, Zonta et al. (33) used artificial CSF equilibrated with 95% O_2, which is a condition that is dramatically different from ours (20%) and favors production of the smooth muscle constrictor 20-HETE (4, 6, 7). This may mask the vasodilatory effects of D-serine and NMDA receptors, making the models difficult to compare appropriately. The cellular source of NMDA receptors responsible for vasodilation in our model is not clear. Our previous work indicates that brain arterial endothelial cells express NMDA receptors capable of initiating a vasodilatory response to extraluminally applied glutamate and D-serine (32). Current data indicate that eNOS contributes to astrocyte-mediated vasodilation and that TTX-sensitive neuronal Na^+ channels, and therefore direct vessel innervation (38), are not required for vasodilation downstream of astrocyte activation. All of these observations tempt speculation that endothelial, rather than neuronal, NMDA receptors participate in astrocyte-mediated vasodilation, but definitive experiments have yet to be performed.

A clear conclusion drawn from our current findings is that eNOS participates in astrocyte-mediated dilation of penetrating cortical arterioles. NO is central to NMDA receptor-mediated neurovascular coupling (10, 39, 40), but only a role for nNOS, specifically, has been described (14, 39, 41). Our finding that a mixture of glutamate or NMDA and D-serine can dilate isolated cerebral arteries by an endothelium and eNOS-dependent mechanism (32) gave rise to the hypothesis that eNOS may be involved in vasodilation initiated by astrocyte gliotransmission in situ. In support of this hypothesis, cortical vasodilation induced by astrocyte Ca^{2+} uncaging was significantly inhibited by L-NIO at a concentration (3 μM) yielding strong selectivity for eNOS (42, 43) and by genetic eNOS deletion. D-serine was also linked directly to eNOS activity in cortical slice arterioles, as L-NIO inhibited vasodilation induced by exogenous application of glutamate/D-serine (10 μM each) in the presence of TTX. In functional hyperemia in vivo, a recent cat study concluded that both nNOS and eNOS participate in vasodilatory responses, with eNOS becoming more prominent at lower levels of neuronal activity and nNOS dominating at higher neuronal activation levels (44). We did not compare the relative roles of eNOS and nNOS in cortical vasodilation induced by *t*ACPD or direct astrocyte activation. Further studies targeting eNOS and nNOS loss of function will assist in determining the relative roles of these isoforms and the cell types in which they are expressed.

Our *t*ACPD and astrocyte Ca^{2+} uncaging paradigms closely resemble those used in several previous studies demonstrating the astrocyte-mediated cortical or hippocampal vasodilation is mediated by the COX metabolite PGE_2 (5–7, 33). Therefore, it is important to address how discovery of a role for eNOS fits with the established COX-mediated mechanism. We found agreement with previous studies (5–7) by showing that COX metabolites also contributed to astrocyte-mediated vasodilation, as INM inhibited vascular responses to Ca^{2+} uncaging. Addition of INM to L-NIO treatment resulted in a loss of vasodilatory effect greater than that achieved with L-NIO alone and actually produced smooth muscle constriction, suggesting that eNOS and COX pathways are additive. Additivity is further supported by the observation that astrocyte-activated eNOS has no direct effect on PGE_2 levels (Fig. 5*C*). It has been reported that NO modulates the vascular effects of AA metabolites by inhibiting cytochrome P450 enzymes that produce 20-HETE and EETs (4). In our hands, cortical 20-HETE content in response to *t*ACPD treatment was significantly enhanced in $eNOS^{-/-}$ slices. This demonstrates that eNOS-derived NO inhibits 20-HETE production and suggests that vasodilation may result from NO-induced suppression of the 20-HETE influence on smooth muscle tone. Support for functional suppression of the vascular effects of 20-HETE comes from experiments using L-NIO and an inhibitor of CYP4A ω-hydroxylase (HET0016), which is the enzyme responsible for 20-HETE formation. The ability of L-NIO to attenuate vasodilatory responses to astrocyte Ca^{2+} uncaging was lost in the presence of HET0016, suggesting that the vasodilatory role of eNOS-derived NO depends on an active 20-HETE production pathway. Overall, our data support dual astrocyte-mediated vasodilatory mechanisms working together. We and others demonstrated that astrocyte activation leads to direct COX-dependent, PGE_2-mediated increases in cortical arteriole lumen diameter. Our data support the idea that astrocyte activation also leads to eNOS activity and suppression of 20-HETE levels, thus facilitating the direct PGE_2-mediated vasodilation.

Materials and Methods

Chemicals and Animals. All chemicals were purchased from Sigma-Aldrich, unless otherwise noted. Animal procedures were approved by the Office of Research Ethics and Compliance Animal Care Committee for the Bannatyne Campus, University of Manitoba. SR deletion mice were generated from C57BL/6-derived embryonic stem cells transfected with the gene-targeting vector containing C57BL/6 mouse genomic DNA and were expanded by crossing with C57BL/6 mice (45). Wild-type littermate controls were used for experiments comparing control to SR knockout phenotypes. eNOS deletion mice were purchased from Jackson Laboratories and bred at the R.O. Burrell Lab at St. Boniface Hospital Research. C57BL/6 was used as the control strain.

Brain Slice Preparation and Two-Photon Laser Scanning Microscopy. Brains from CD1 or C57BL/6 mice (14–19 d old) were placed in ice-cold cutting buffer (2.5 mM KCl, 1.25 mM NaH_2PO_4, 10 mM $MgSO_4$, 5 mM $CaCl_2$, 26 mM $NaHCO_3$, 10 mM glucose, 230 mM sucrose) bubbled with 95% O_2 and 5% CO_2. Slices were cut on a vibrating blade microtome (350 μm) and were then maintained in aCSF (126 mM NaCl, 2.5 mM KCl, 1.25 mM NaH_2PO_4, 2 mM $MgCl_2$, 2 mM $CaCl_2$, 26 mM $NaHCO_3$, 10 mM glucose) equilibrated with 95% O_2, 5% CO_2, and heated to 35 °C. After 1 h, slices were loaded with the Ca^{2+} indicator dye, Rhodamine-2 AM (10 μM; Invitrogen), and *Griffonia simplicifolia* 1 Isolectin B_4 tagged with Alexa Fluor 488 (5 μg/mL; Invitrogen). Two-photon imaging proceeded on the stage of an upright microscope in aCSF equilibrated with 20% O_2, 5% CO_2, and 75% N_2. Scans were performed using an excitation wavelength of 800 nm, delivered through an Ultima multiphoton scanhead, with dual galvanometers for imaging and uncaging (Prairie Technologies), by a pulsed Ti-sapphire laser (Coherent Inc.). For astrocyte Ca^{2+} uncaging, cortical slices were incubated with o-nitrophenyl-EGTA AM (10 μM; Invitrogen) for 1 h. Cytoplasmic photoliberation of Ca^{2+} was achieved using functional mapping software (TriggerSync, Prairie Technologies) to guide a 700 nm/100 ms laser pulse through a voltage-controlled pockels cell. Images were analyzed every 15 s using PrairieView software to determine vessel lumen diameter, as marked by isolectin staining. Changes in vessel lumen diameter were correlated with astrocyte rhodamine-2 Ca^{2+} fluorescence intensity changes, which were measured using ImageJ.

D-Serine and Glutamate Release Assays. Acute brain slices were incubated in aCSF equilibrated with 20% O_2/5% CO_2 and then stimulated with *t*ACPD (100 μM) for 15 min. Some slices were pretreated with DAAO (0.1 U/mL) or TTX (1 μM) for 20 min. During *t*ACPD stimulation, samples of aCSF were collected at 0 min, 5 min, or 15 min for measurement of D-serine and glutamate concentrations. D-serine release was measured by chemiluminescent assay, as described previously with minor modification (46, 47). We mixed 10 μl of each sample with 100 μl of aCSF containing 100 mM Tris-HCl, pH 8.8, 20 U/mL peroxidase, and 8 μl of luminol. Samples were incubated 15 min to decrease background signal of luminol, and then 10 μl of DAAO (75 U/mL) was added, where applicable. Chemiluminescence kinetics was recorded for 5 min at room temperature using a TD-20/20 Luminometer (Turner Designs). D-serine concentrations were calculated based on a standard curve. Glutamate release was determined at each time point by using Amplex Red Glutamic Acid/Glutamate Oxidase Assay Kit (Invitrogen).

PGE_2 and 20-HETE ELISAs. Acute brain slices were incubated in aCSF equilibrated with 20% O_2/5% CO_2 and stimulated with *t*ACPD (100 μM) for 5 min. Some slices were pretreated with TTX (1 μM) with or without L-NIO (3 μM) for 20 min. PGE_2 release in aCSF was measured using the PGE_2 enzyme immunoassay (EIA) Kit (Cayman). For 20-HETE, brain slices were lysed and 20-HETE production was measured by 20-HETE ELISA Kit (Detroit R&D, Inc.).

D-Serine Immunohistochemistry. D-serine immunostaining was modified from the procedure by Schell et al. (1995) (26). Brains from 14–19-d-old CD1 mice were fixed (5% glutaraldehyde, 0.5% PFA, 0.2% $Na_2S_2O_5$, 0.1 M Na_2PO_4 buffer at pH 7.4) for 24 h and cryopreserved in 30% sucrose. Tissue was then snap-frozen in liquid nitrogen cooled n-hexane and cut into 30 μm sections. Slices were reduced for 20 min at room temperature in 0.2% $Na_2S_2O_5$ and 0.5% $NaBH_4$ in 0.1 M Tris-buffered saline (TBS; pH 7.4) and rinsed with 0.2% $Na_2S_2O_5$ in TBS for 45 min. Tissue was blocked in 4% goat serum, 0.2% Triton X-100, and 0.2% $Na_2S_2O_5$ in 0.1 M TBS for 2 h and then incubated in 0.1 M TBS (pH 7.2) with 2% goat serum, 0.1% Triton X-100, and primary antibodies: rabbit anti-D-serine (Millipore), mouse anti-GFAP, and *G. simplicifolia* 1 Isolectin B_4 tagged with Alexa Fluor 488 (Invitrogen) for 48 h. Secondary antibodies Alexa Fluor 633 goat anti-rabbit IgG (H+L) (Invitrogen) and Alexa Fluor 568 goat anti-mouse IgG (H+L) (Invitrogen) were used for visualization of D-serine and GFAP. Images were collected with a Zeiss LSM510 laser-scanning microscope.

Data Analysis. AUC was calculated from percent vessel relaxation versus time plots. AUC among experimental groups were compared using *t* test for two groups or one-way ANOVA with Student Newman–Keuls post hoc test for three or more groups. The time course of glutamate and D-serine release from slices was analyzed by two-way ANOVA with Bonferroni post hoc tests.

ACKNOWLEDGMENTS. The authors thank Ms. Ayumi Tanaka for SR deletion mouse preparation. Research was supported by an operating grant from the Canadian Institutes of Health Research. J.L.S. was supported by a student award from the Canadian Institutes of Health Research.

1. Iadecola C (2004) Neurovascular regulation in the normal brain and in Alzheimer's disease. *Nat Rev Neurosci* 5(5):347–360.
2. Filosa JA, et al. (2006) Local potassium signaling couples neuronal activity to vasodilation in the brain. *Nat Neurosci* 9(11):1397–1403.
3. Girouard H, et al. (2010) Astrocytic endfoot Ca2+ and BK channels determine both arteriolar dilation and constriction. *Proc Natl Acad Sci USA* 107(8):3811–3816.
4. Metea MR, Newman EA (2006) Glial cells dilate and constrict blood vessels: A mechanism of neurovascular coupling. *J Neurosci* 26(11):2862–2870.
5. Takano T, et al. (2006) Astrocyte-mediated control of cerebral blood flow. *Nat Neurosci* 9(2):260–267.
6. Mishra A, Hamid A, Newman EA (2011) Oxygen modulation of neurovascular coupling in the retina. *Proc Natl Acad Sci USA* 108(43):17827–17831.
7. Gordon GR, Choi HB, Rungta RL, Ellis-Davies GC, MacVicar BA (2008) Brain metabolism dictates the polarity of astrocyte control over arterioles. *Nature* 456(7223):745–749.
8. Mulligan SJ, MacVicar BA (2004) Calcium transients in astrocyte endfeet cause cerebrovascular constrictions. *Nature* 431(7005):195–199.
9. Busija DW, Leffler CW (1989) Dilator effects of amino acid neurotransmitters on piglet pial arterioles. *Am J Physiol* 257(4 Pt 2):H1200–H1203.
10. Faraci FM, Breese KR (1993) Nitric oxide mediates vasodilatation in response to activation of N-methyl-D-aspartate receptors in brain. *Circ Res* 72(2):476–480.
11. Bhardwaj A, et al. (2000) P-450 epoxygenase and NO synthase inhibitors reduce cerebral blood flow response to N-methyl-D-aspartate. *Am J Physiol Heart Circ Physiol* 279(4):H1616–H1624.
12. Simandle SA, et al. (2005) Piglet pial arteries respond to N-methyl-D-aspartate in vivo but not in vitro. *Microvasc Res* 70(1–2):76–83.
13. Iadecola C (1993) Regulation of the cerebral microcirculation during neural activity: Is nitric oxide the missing link? *Trends Neurosci* 16(6):206–214.
14. Fergus A, Lee KS (1997) Regulation of cerebral microvessels by glutamatergic mechanisms. *Brain Res* 754(1–2):35–45.
15. Ma J, Ayata C, Huang PL, Fishman MC, Moskowitz MA (1996) Regional cerebral blood flow response to vibrissal stimulation in mice lacking type I NOS gene expression. *Am J Physiol* 270(3 Pt 2):H1085–H1090.
16. Alonso-Galicia M, Hudetz AG, Shen H, Harder DR, Roman RJ (1999) Contribution of 20-HETE to vasodilator actions of nitric oxide in the cerebral microcirculation. *Stroke* 30(12):2727–2734, discussion 2734.
17. Liu X, et al. (2008) Interaction of nitric oxide, 20-HETE, and EETs during functional hyperemia in whisker barrel cortex. *Am J Physiol Heart Circ Physiol* 295(2):H619–H631.
18. Ma J, et al. (1996) L-NNA-sensitive regional cerebral blood flow augmentation during hypercapnia in type III NOS mutant mice. *Am J Physiol* 271(4 Pt 2):H1717–H1719.
19. Pereira de Vasconcelos A, Riban V, Wasterlain C, Nehlig A (2006) Role of endothelial nitric oxide synthase in cerebral blood flow changes during kainate seizures: A genetic approach using knockout mice. *Neurobiol Dis* 23(1):219–227.
20. Hlatky R, et al. (2003) The role of endothelial nitric oxide synthase in the cerebral hemodynamics after controlled cortical impact injury in mice. *J Neurotrauma* 20(10):995–1006.
21. Endres M, Laufs U, Liao JK, Moskowitz MA (2004) Targeting eNOS for stroke protection. *Trends Neurosci* 27(5):283–289.
22. Dingledine R, Borges K, Bowie D, Traynelis SF (1999) The glutamate receptor ion channels. *Pharmacol Rev* 51(1):7–61.
23. Fadda E, Danysz W, Wroblewski JT, Costa E (1988) Glycine and D-serine increase the affinity of N-methyl-D-aspartate sensitive glutamate binding sites in rat brain synaptic membranes. *Neuropharmacology* 27(11):1183–1185.
24. Matsui T, et al. (1995) Functional comparison of D-serine and glycine in rodents: The effect on cloned NMDA receptors and the extracellular concentration. *J Neurochem* 65(1):454–458.
25. Shleper M, Kartvelishvily E, Wolosker H (2005) D-serine is the dominant endogenous coagonist for NMDA receptor neurotoxicity in organotypic hippocampal slices. *J Neurosci* 25(41):9413–9417.
26. Schell MJ, Molliver ME, Snyder SH (1995) D-serine, an endogenous synaptic modulator: Localization to astrocytes and glutamate-stimulated release. *Proc Natl Acad Sci USA* 92(9):3948–3952.
27. Wolosker H, Blackshaw S, Snyder SH (1999) Serine racemase: A glial enzyme synthesizing D-serine to regulate glutamate-N-methyl-D-aspartate neurotransmission. *Proc Natl Acad Sci USA* 96(23):13409–13414.
28. Mothet JP, et al. (2005) Glutamate receptor activation triggers a calcium-dependent and SNARE protein-dependent release of the gliotransmitter D-serine. *Proc Natl Acad Sci USA* 102(15):5606–5611.
29. Panatier A, et al. (2006) Glia-derived D-serine controls NMDA receptor activity and synaptic memory. *Cell* 125(4):775–784.
30. Henneberger C, Papouin T, Oliet SH, Rusakov DA (2010) Long-term potentiation depends on release of D-serine from astrocytes. *Nature* 463(7278):232–236.
31. Yang Y, et al. (2003) Contribution of astrocytes to hippocampal long-term potentiation through release of D-serine. *Proc Natl Acad Sci USA* 100(25):15194–15199.
32. LeMaistre JL, et al. (2012) Coactivation of NMDA receptors by glutamate and D-serine induces dilation of isolated middle cerebral arteries. *J Cereb Blood Flow Metab* 32(3):537–547.
33. Zonta M, et al. (2003) Neuron-to-astrocyte signaling is central to the dynamic control of brain microcirculation. *Nat Neurosci* 6(1):43–50.
34. Martineau M, Galli T, Baux G, Mothet JP (2008) Confocal imaging and tracking of the exocytotic routes for D-serine-mediated gliotransmission. *Glia* 56(12):1271–1284.
35. Rosenberg D, et al. (2010) Neuronal release of D-serine: A physiological pathway controlling extracellular D-serine concentration. *FASEB J* 24(8):2951–2961.
36. Roman RJ (2002) P-450 metabolites of arachidonic acid in the control of cardiovascular function. *Physiol Rev* 82(1):131–185.
37. Koide M, Bonev AD, Nelson MT, Wellman GC (2012) Inversion of neurovascular coupling by subarachnoid blood depends on large-conductance Ca^{2+}-activated K^+ (BK) channels. *Proc Natl Acad Sci USA* 109(21):E1387–E1395.
38. Tong XK, Hamel E (2000) Basal forebrain nitric oxide synthase (NOS)-containing neurons project to microvessels and NOS neurons in the rat neocortex: Cellular basis for cortical blood flow regulation. *Eur J Neurosci* 12(8):2769–2780.
39. Bari F, Errico RA, Louis TM, Busija DW (1996) Interaction between ATP-sensitive K^+ channels and nitric oxide on pial arterioles in piglets. *J Cereb Blood Flow Metab* 16(6):1158–1164.
40. Meng W, Tobin JR, Busija DW (1995) Glutamate-induced cerebral vasodilation is mediated by nitric oxide through N-methyl-D-aspartate receptors. *Stroke* 26(5):857–862, discussion 863.
41. Faraci FM, Brian JE, Jr. (1995) 7-Nitroindazole inhibits brain nitric oxide synthase and cerebral vasodilatation in response to N-methyl-D-aspartate. *Stroke* 26(11):2172–2175, discussion 2176.
42. Chinellato A, Froldi G, Caparrotta L, Ragazzi E (1998) Pharmacological characterization of endothelial cell nitric oxide synthase inhibitors in isolated rabbit aorta. *Life Sci* 62(6):479–490.
43. Rees DD, Palmer RM, Schulz R, Hodson HF, Moncada S (1990) Characterization of three inhibitors of endothelial nitric oxide synthase in vitro and in vivo. *Br J Pharmacol* 101(3):746–752.
44. de Labra C, et al. (2009) Different sources of nitric oxide mediate neurovascular coupling in the lateral geniculate nucleus of the cat. *Front Syst Neurosci* 3:9.
45. Miya K, et al. (2008) Serine racemase is predominantly localized in neurons in mouse brain. *J Comp Neurol* 510(6):641–654.
46. Wolosker H, et al. (1999) Purification of serine racemase: Biosynthesis of the neuromodulator D-serine. *Proc Natl Acad Sci USA* 96(2):721–725.
47. Zhuang Z, et al. (2010) EphrinBs regulate D-serine synthesis and release in astrocytes. *J Neurosci* 30(47):16015–16024.

Epilepsy & Behavior 24 (2012) 373–376

Contents lists available at SciVerse ScienceDirect

Epilepsy & Behavior

journal homepage: www.elsevier.com/locate/yebeh

Case Report

Acute psychosis during the postictal period in a patient with idiopathic generalized epilepsy: Postictal psychosis or aggravation of schizophrenia? A case report and review of the literature

Eisuke Sakakibara [a,b,*], Takuji Nishida [b,c], Kazuyuki Sugishita [b,d], Seiichiro Jinde [b], Yushi Inoue [c], Kiyoto Kasai [b]

[a] Department of Psychiatry, National Center of Neurology and Psychiatry, National Center Hospital, Japan
[b] Department of Neuropsychiatry, The University of Tokyo Hospital, Japan
[c] National Epilepsy Center, Shizuoka Institute of Epilepsy and Neurological Disorders, Japan
[d] Oji Mental Clinic, Japan

ARTICLE INFO

Article history:
Received 2 April 2012
Revised 10 April 2012
Accepted 21 April 2012
Available online 29 May 2012

Keywords:
Psychotic disorders
Postictal psychosis
Interictal psychosis
Epilepsy
Idiopathic generalized epilepsy
Schizophrenia

ABSTRACT

Postictal psychoses are common comorbid conditions of temporal lobe epilepsy and are reported to be characterized by affective changes. However, postictal psychoses are rare among patients with idiopathic generalized epilepsy, and the causal relationship between postictal psychoses and idiopathic generalized epilepsy is unknown. Here, we report the case of a man who had idiopathic generalized epilepsy and experienced 4 episodes of schizophrenia-like interictal psychosis before the age of 41 years. At the age of 56 years, he experienced a generalized tonic-clonic seizure for the first time in 15 years and developed psychotic symptoms on the next day. Notably, in addition to the schizophrenia-like symptoms, the patient experienced mania-like symptoms such as elated mood, grandiose delusions, agitation, and pressured speech during the last psychotic episode in the postictal period. It was suspected that postictal neuronal processes and a predisposition to endogenous psychosis both contributed to the psychopathology of this episode.

1. Introduction

Although the association between epilepsy and psychosis has been noted since the mid-nineteenth century, the role of seizures in the pathogenesis of psychoses in patients with epilepsy and whether epileptic psychosis and endogenous psychosis, such as schizophrenia, are the same are unknown [1–3]. Psychoses, comorbid with epilepsy, are classified according to the temporal relationship between seizure and psychosis and according to the type of epilepsy. Many studies have focused on the heterogeneity of epileptic psychoses [4–7]. Postictal psychosis is a type of epileptic psychosis that presents within a week of a seizure or a cluster of seizures and is known to be associated with temporal lobe epilepsy (TLE); however, this condition is rare among patients with idiopathic generalized epilepsy (IGE) [4,5,8–11]. Previous studies have documented that affective changes are frequently observed during postictal psychoses [10–12], and a case–control study indicated that postictal psychoses have a greater number of mania-like symptoms rather than schizophrenia-like symptoms, whereas interictal psychoses have a greater number of schizophrenia-like symptoms [4]. Our case report describes the case of a patient who had IGE and experienced 4 episodes of schizophrenia-like interictal psychosis before the age of 41 years. He did not experience any seizures or psychotic episodes from the age of 41 years to 56 years. At the age of 56 years, he experienced a generalized tonic-clonic seizure, which was followed by acute psychosis during the postictal stage; the psychosis was characterized by both schizophrenia-like and mania-like symptoms. In light of these findings, we have reviewed the current literature on epilepsy and postictal psychoses.

2. Case report

Informed consent was obtained from the patient and his family for this case report, and details that might disclose the identity of the patient have been omitted. The patient was a right-handed 56-year-old man with a history of febrile seizures; his first generalized convulsion occurred at 7 years of age. Although phenobarbital was administered subsequently, he experienced generalized tonic-clonic seizures not accompanied by aura a few times a year. He was a good student in high school, and he majored in science from one of the most prestigious universities in Japan. In his early twenties, he gradually became

* Corresponding author at: Department of Psychiatry, National Center of Neurology and Psychiatry, National Center Hospital, 4-1-1, Ogawa-Higashi, Kodaira, Tokyo 187-8551, Japan. Fax: +81 42 344 6745.
E-mail address: sakakibara-tky@umin.ac.jp (E. Sakakibara).

1525-5050/$ – see front matter © 2012 Elsevier Inc. All rights reserved.
doi:10.1016/j.yebeh.2012.04.127

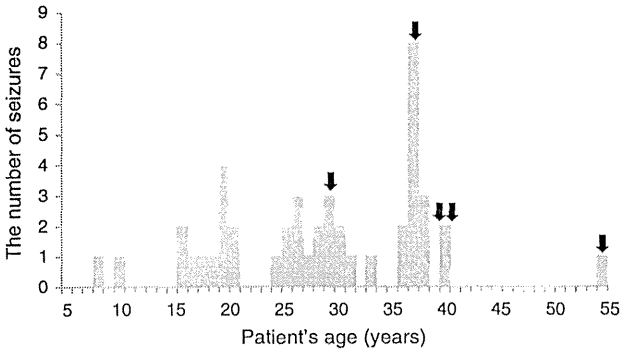

Fig. 1. Seizure frequency and psychotic episodes. Black arrows designate the episodes of psychosis.

suspicious that his seizures were the result of an assault by someone. After graduating from university, he became a high school teacher at the age of 26. At the age of 30 years, he experienced financial issues. While he was concerned with the dispute, his suspiciousness developed into a persecutory delusion that he had been attacked with high-frequency waves by an "offender;" consequently, he was hospitalized for 3 weeks at 31 years of age. The seizure frequencies are illustrated in Fig. 1.

After this first psychotic episode, he returned to work as a high school teacher and continued teaching until 38 years of age when a psychotic episode characterized by persecutory delusions, auditory hallucinations, including hearing the commanding voice of the "offender," and disorganized behavior occurred. He was unwilling to take antiepileptics. When the frequency of seizures reached as many as 8 per year, he was referred to an epilepsy center in Japan. Electroencephalogram (EEG) showed a very rare synchronized symmetrical bilateral diffuse spike-and-wave during the sleeping state (Fig. 2). His epilepsy was diagnosed as IGE on the basis of the clinical semiology of seizures and EEG findings. Subsequently, 400 mg/day of valproate and 4 mg/day of haloperidol were administered, which greatly reduced the frequency of seizures and resolved the psychosis. He experienced acute schizophrenia-like psychoses, characterized by delusion and hallucination, at the ages of 40 and 41; each episode remitted within 1 month without hospitalization. All these psychotic episodes occurred at > 1-month interval from the nearest past seizures.

After the fourth psychotic episode, his seizures remitted and psychosis was not observed. He stopped working as a regular teacher at the age of 47 years and helped his family on their farm later; he did not marry. He has a strong family history of psychiatric illness among his first-degree relatives; his younger brother has epilepsy, acute transient psychosis, and mild retardation; his father was diagnosed with depression and committed suicide.

At the age of 56 years, he once attended to his mother overnight when she was sick. The next morning, he experienced a generalized tonic-clonic seizure for the first time in 15 years. On the next day, he began complaining about various somatic discomforts, including pain in his penis. He visited several physicians and surgeons, but no objective abnormalities were detected. Five days after the seizure, he began to hear the voice of the "offender," who directed him to "make emergency calls to police." His family witnessed his conversations with the voices. Because increasing the dosage of antipsychotics was ineffective, he was involuntarily hospitalized 21 days after the seizure. On admission, the patient was markedly elated, agitated, and talkative. Persecutory delusion, grandiose delusion, and conversations with voices were observed. He refused psychiatric examination and began shouting, for example, "I am the president of X University" and "I can receive air wave because the receiver has been implanted in my brain." He also complained that his penis was made painful by the "offender." Neurological examinations, laboratory data, computed tomography (CT), and magnetic resonance imaging (MRI) of the head showed no abnormality. EEG taken on admission showed 11 Hz, 50–100 μV, well-organized bi-occipital dominant α rhythm at rest with no paroxysmal discharge.

Treatment with intravenous haloperidol was initiated. By the third week of hospitalization, elated mood, agitation, pressured speech, and grandiose delusion had remitted; therefore, intravenous haloperidol was gradually replaced with oral haloperidol (~36 mg/day) and levomepromazine (~125 mg/day). By the seventh week of hospitalization, the auditory hallucinations and persecutory delusions had almost resolved. However, avolition and psychomotor inhibition became prominent, because of which the dosage of antipsychotics was changed to 4.5 mg/day of haloperidol and 125 mg/day of chlorpromazine. The patient was discharged 115 days after the admission. At the time of discharge, he had no current hallucinations or delusions, although he lacked insight that the voices he previously heard were hallucinations.

The Young Mania Rating Scale (YMRS) [13] and Positive and Negative Syndrome Scale (PANSS) [14] were evaluated weekly during the hospitalization. Fig. 3 illustrates the changes in YMRS scores and the positive and negative scales of PANSS. EEGs were performed repeatedly, but paroxysmal discharge was undetected. The results of the Wechsler Adult Intelligence Scale – Revised (WAIS-R) indicated borderline intelligence with significant decrease in performance intelligence quotient (IQ) relative to verbal IQ (full scale IQ, 80; verbal IQ, 92; performance IQ, 69).

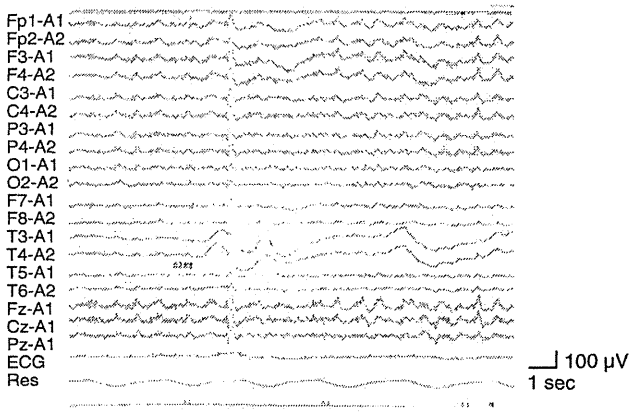

Fig. 2. An electroencephalogram taken at 39 years of age. Bilateral diffuse spike-and-wave was recorded.

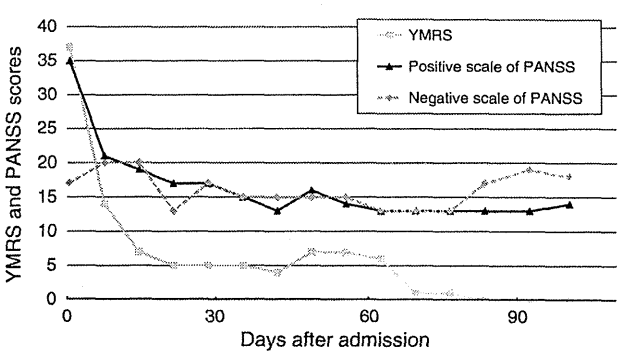

Fig. 3. Young Mania Rating Scale (YMRS) scores and positive and negative scale scores of Positive and Negative Syndrome Scale (PANSS) during hospitalization.

Table 1
Comparison of symptoms between interictal psychosis and postictal psychosis.
Adapted from [4,11,16,17].

	Postictal psychosis	Interictal psychosis	The present case
General feature	Mania-like	Schizophrenia-like	The mixture of both
Delusion	Grandiose, religious	Persecutory, referential	Grandiose, persecutory
First-rank symptoms	Rare	Common	Exist
Aggression, pressured speech, excessive emotional response	Common	Rare	Exist
Temporal relation to seizure	Mostly within 72 h after seizure	Unclear	Next day
Period of psychosis	Mostly within a month	Longer than postictal psychosis	2 months

3. Discussion

To understand the association between epilepsy and psychosis, both the specific type of epileptic syndrome and the temporal relationship between seizure and psychosis need to be considered.

3.1. Psychoses and specific epileptic syndromes

Psychoses are often seen among patients with localization-related epilepsy, especially TLE, which may be caused by dysfunctions of the temporal lobe and limbic system related to organic lesions and epileptic discharge [2]. On the other hand, psychoses are rarely seen in patients with IGE. A study reported that psychiatric symptoms were observed in 19.4% of 67 patients with IGE, most of which were episodic disturbances in behavior such as sexually aberrant activities; only 2 experienced auditory hallucinations and 1 experienced delusion [6]. Currently, there are no data on the correlation between IGE and schizophrenia-like psychosis. Adachi and colleagues found that the onset of psychosis in patients with generalized epilepsies is significantly earlier than that in patients with localization-related epilepsies (22.5 ± 1.0 years of age vs. 29.1 ± 0.7 years of age), and this onset is more comparable to what is seen in patients with schizophrenia [7]. Predisposed vulnerabilities to psychosis may contribute to the incidence of psychosis in patients with IGE, whereas epilepsy-related damage appears to be more relevant to psychoses in patients with localization-related epilepsy.

3.2. Interictal psychosis and postictal psychosis

The second important distinction to be considered is the temporal relationship between seizure and psychosis. Psychoses occurring in conjunction with or soon after a seizure or cluster of seizures indicate a positive relationship between seizure and psychosis. Another interesting case is alternating psychoses in which seizures and psychoses are observed in alternation [15]. When no such temporal link is observed, no direct relation is considered between seizures and psychoses.

Postictal psychosis was defined by Logsdail and Toone as a psychotic episode that occurs within a week of the last epileptic seizure and can last from 24 h to 3 months [8]. These authors excluded patients with a history of psychoses unassociated with seizures, and most subsequent studies on postictal psychosis have followed this definition of postictal psychosis [4,9,10,12]. Therefore, strictly speaking, the last episode of psychosis in the present case does not meet criteria for postictal psychosis as per this definition. However, it may be of some benefit to compare the present case with the examples of postictal psychoses documented in the literature. Adachi and colleagues have identified patients with epilepsy who have experienced acute psychoses during both the postictal and interictal periods [5,16] and have proposed the clinical entity of "bimodal psychosis" for this condition. The present case also comes under the parameters of bimodal psychosis.

Kanemoto and colleagues compared interictal psychosis and postictal psychosis among patients with TLE and noted differences in the symptoms of these 2 types of psychoses [4]. As shown in Table 1, interictal psychoses are more schizophrenia-like, in that first-rank symptoms (Schneider K) are more common and delusions are typically persecutory or referential. In contrast, postictal psychoses are more mania-like, where elated mood, aggression, pressured speech, and excessive emotional response are prominent and delusions are typically grandiose or religious. It is also known that seizures are sometimes followed by full-fledged manic episodes [18,19].

3.3. Postictal psychosis in IGE

Postictal psychoses are found more often in patients with localization-related epilepsy than in patients with IGE. The prevalence rates of postictal psychoses are reported to be from 3.7% [4] to 6.4% [12] in patients with TLE. Although rare, postictal psychoses have also been reported in patients with IGE [8,10,20].

When acute psychosis is observed during the postictal period in a patient with IGE, the question arises whether it is an epilepsy-related psychosis or a coincidence of endogenous psychosis. In the present case, the comorbidity of endogenous psychosis, especially schizophrenia, was suspected because there were 4 episodes of schizophrenia-like psychosis without noticeable temporal proximity to seizures. Evidence of family history of endogenous mental disorders and the apparent gradual decline in social functioning support this hypothesis. On the other hand, because the last psychotic episode began on the day following the seizure that had been dormant for 15 years, it is reasonable to assume that the seizure and the psychosis are related.

One hypothesis is as follows: The patient's family history indicated a predisposition to endogenous psychosis. When the patient was in his thirties and early forties, the propensity for psychosis was not sufficiently high and the seizures did not elicit psychoses. He experienced 4 seizure-unrelated psychotic episodes triggered by psychological burdens, such as financial issues and hardships experienced at work. After he stopped working as a teacher, the propensity for endogenous psychosis had not exceeded the threshold because he lived peacefully and did not experience seizures. However, he was getting progressively vulnerable to psychosis, as suggested by the decrease in IQ scores. At the age of 56 years, the patient's propensity for psychosis was sufficiently high for a seizure to trigger acute psychosis.

It is particularly noteworthy that the latest psychosis during the postictal period showed mania-like symptoms in addition to schizophrenia-like symptoms, whereas all the past 4 psychoses during the interictal periods showed schizophrenia-like symptoms without affective disturbance. This may suggest that both the predisposition to endogenous psychosis and the postictal neuronal process contributed to the psychopathology of the episode during the postictal period.

References

[1] Slater E, Beard AW. The schizophrenia-like psychoses of epilepsy. Br J Psychiatry 1963;109:95–150.
[2] Perez MM, Trimble MR. Epileptic psychosis — diagnostic comparison with process schizophrenia. Br J Psychiatry 1980;137:245–9.

[3] Sachdev P. Schizophrenia-like psychosis and epilepsy: the status of the association. Am J Psychiatry 1998;155:325–36.
[4] Kanemoto K, Kawasaki J, Kawai I. Postictal psychosis: a comparison with acute interictal and chronic psychoses. Epilepsia 1996;37:551–6.
[5] Adachi N, Matsuura M, Hara T, et al. Psychoses and epilepsy: are interictal and postictal psychoses distinct clinical entities? Epilepsia 2002;43:1574–82.
[6] Sengoku A, Toichi M, Murai T. Comparison of psychotic states in patients with idiopathic generalized epilepsy and temporal lobe epilepsy. Epilepsia 1997;38(Suppl. 6): 22–5.
[7] Adachi N, Akanuma N, Ito M, et al. Epileptic, organic and genetic vulnerabilities for timing of the development of interictal psychosis. Br J Psychiatry 2010;196: 212–6.
[8] Logsdail SJ, Toone BK. Postictal psychosis. A clinical and phenomenological description. Br J Psychiatry 1988;152:246–52.
[9] Savard G, Andermann F, Olivier A, Rémillard GM. Postictal psychosis after partial complex seizures: a multiple case study. Epilepsia 1991;32:25–31.
[10] Devinsky O, Abramson H, Alper K, et al. Postictal psychosis: a case control series of 20 patients and 150 controls. Epilepsy Res 1995;20:247–53.
[11] Trimble M, Kanner A, Schmitz B. Postictal psychosis. Epilepsy Behav 2010;19: 159–61.
[12] Kanner AM, Stagno S, Kotagal P, Morris H. Postictal psychiatric events during prolonged video-electroencephalographic monitoring studies. Arch Neurol 1996;53:258–63.
[13] Young RC, Biggs JT, Ziegler VE, Meyer DA. A rating scale for mania: reliability validity and sensitivity. Br J Psychiatry 1978;133:429–35.
[14] Kay SR, Fiszbein A, Opfer LA. The positive and negative syndrome scale (PANSS) for schizophrenia. Schizophr Bull 1987;13:261–76.
[15] Wolf P. Acute behavioral symptomatology at disappearance of epileptiform EEG abnormality. Paradoxical or "forced" normalization. Adv Neurol 1991;55:127–42.
[16] Adachi N, Kato M, Sekimoto M, et al. Recurrent postictal psychosis after remission of interictal psychosis: further evidence of bimodal psychosis. Epilepsia 2003;44: 1218–22.
[17] Adachi N, Ito M, Kanemoto K, et al. Duration of postictal psychotic episodes. Epilepsia 2007;48:1531–7.
[18] Chakrabarti S, Aga VM, Singh R. Postictal mania following primary generalized seizures. Neurol India 1999;47:332–3.
[19] Nishida T, Kudo T, Inoue Y, et al. Postictal mania versus postictal psychosis: differences in clinical features, epileptogenic zone, and brain functional changes during postictal period. Epilepsia 2006;47:2104–14.
[20] Fong GC, Ho WY, Tsoi TH, Fong KY, Ho SL. Lateral temporal hyperperfusion in postictal psychosis assessed by 99mTc-HMPAO SPECT. Neuroimage 2002;17:1634–7.